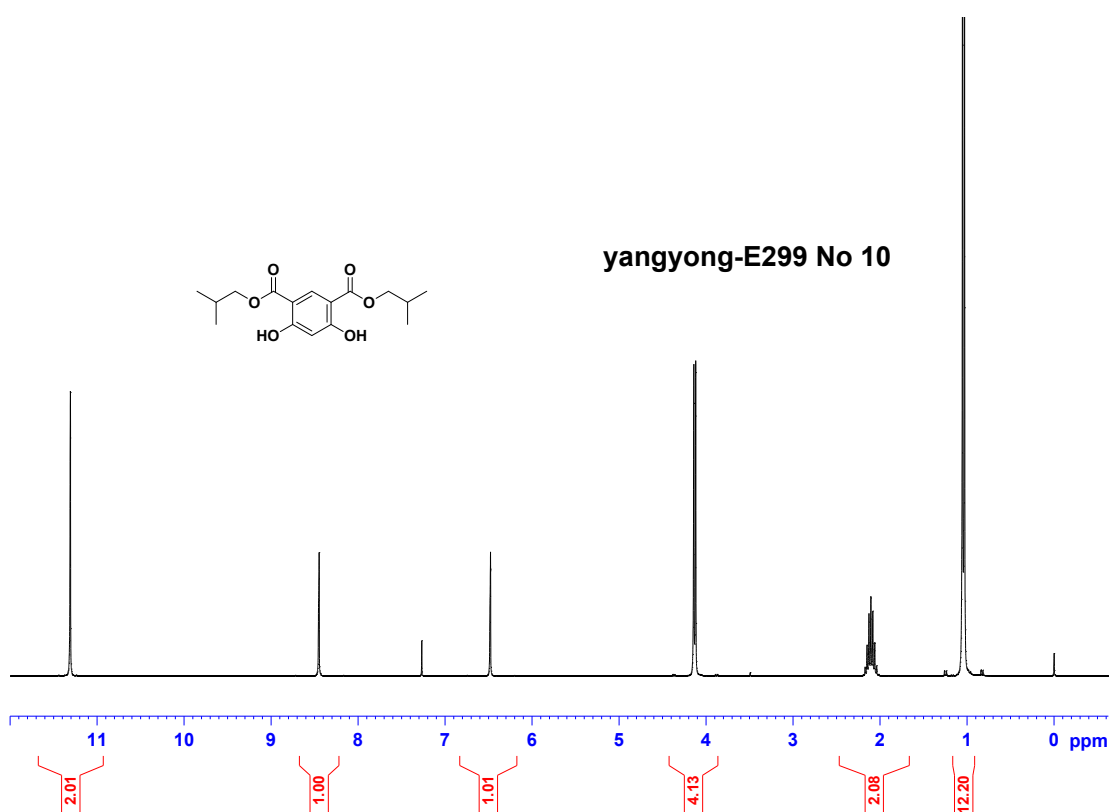
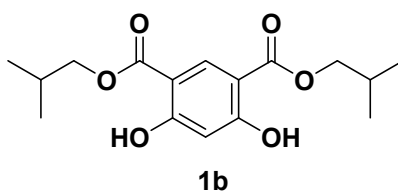


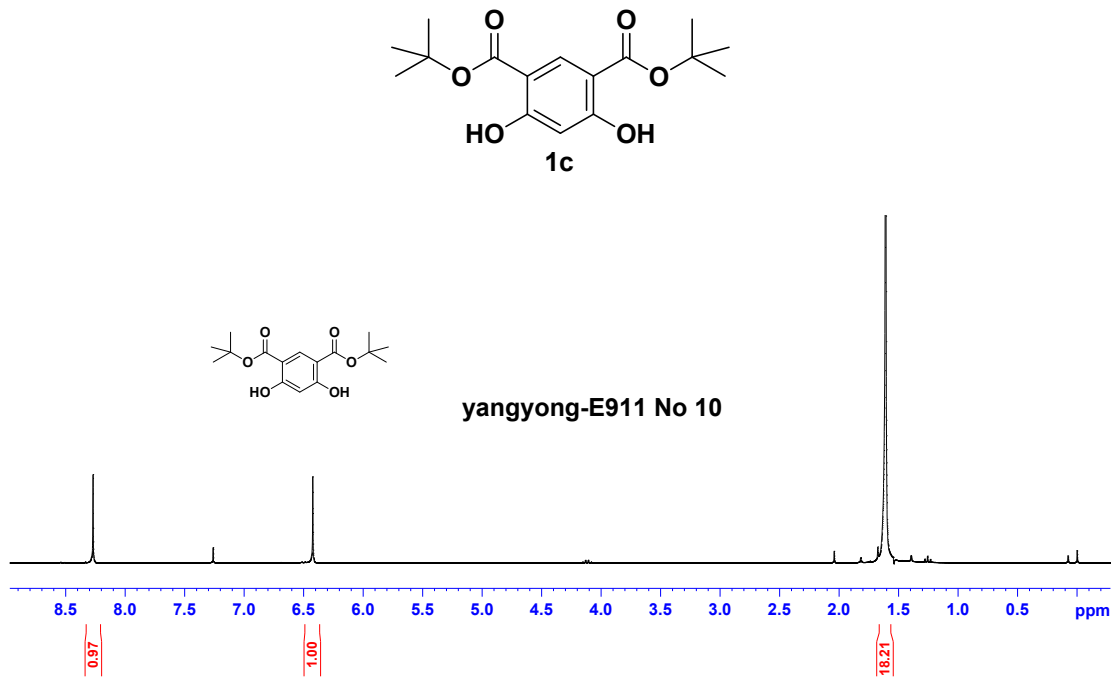
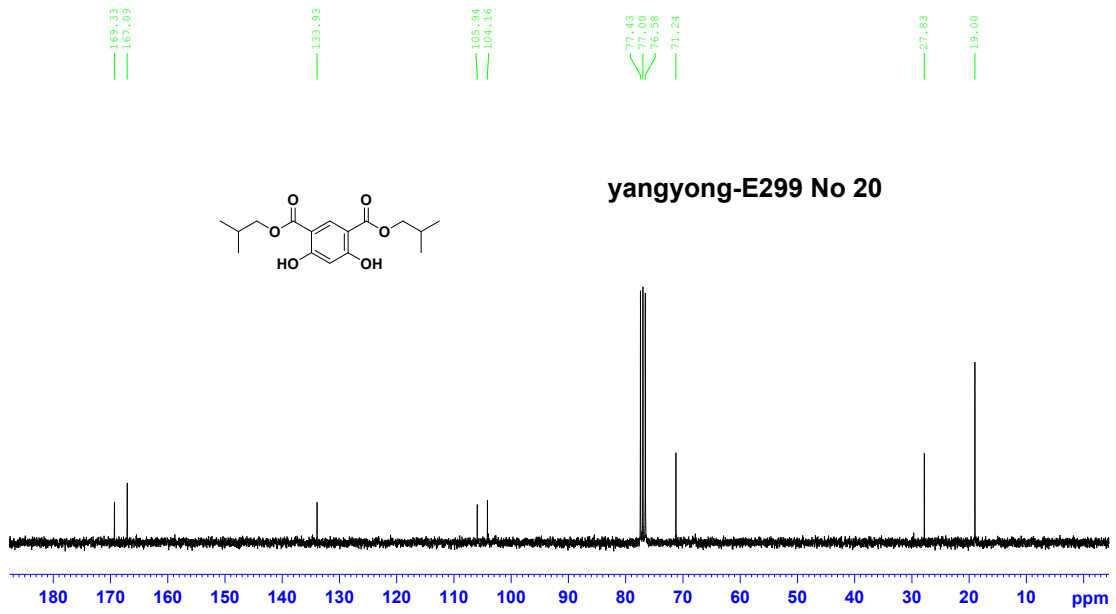
Electronic Supplementary Information

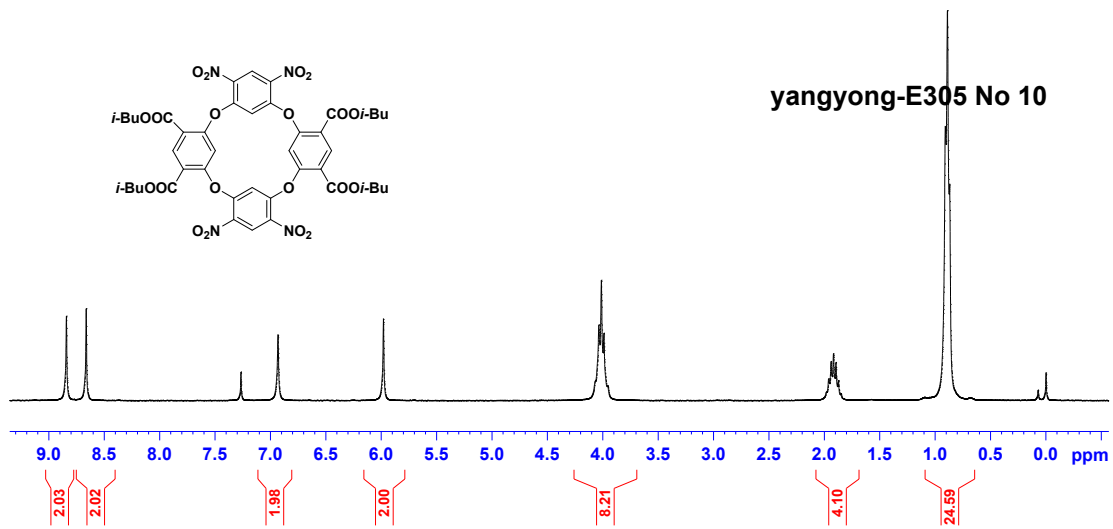
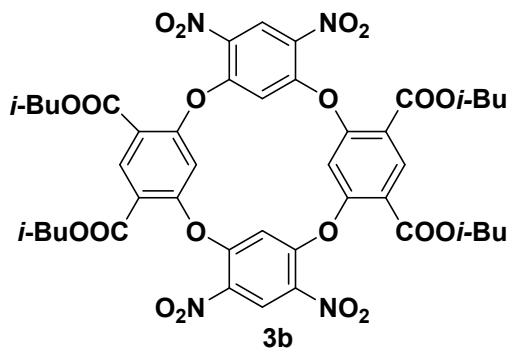
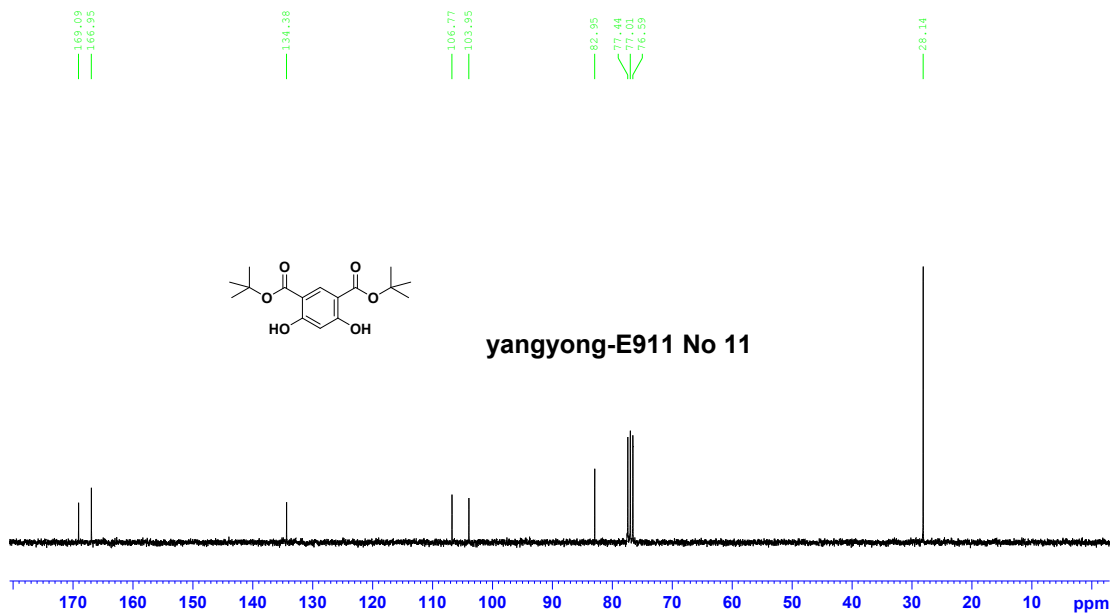
Synthesis, structure, and anion binding of functional oxacalix[4]arenes

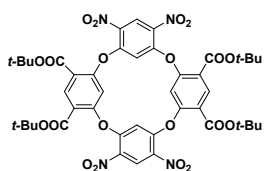
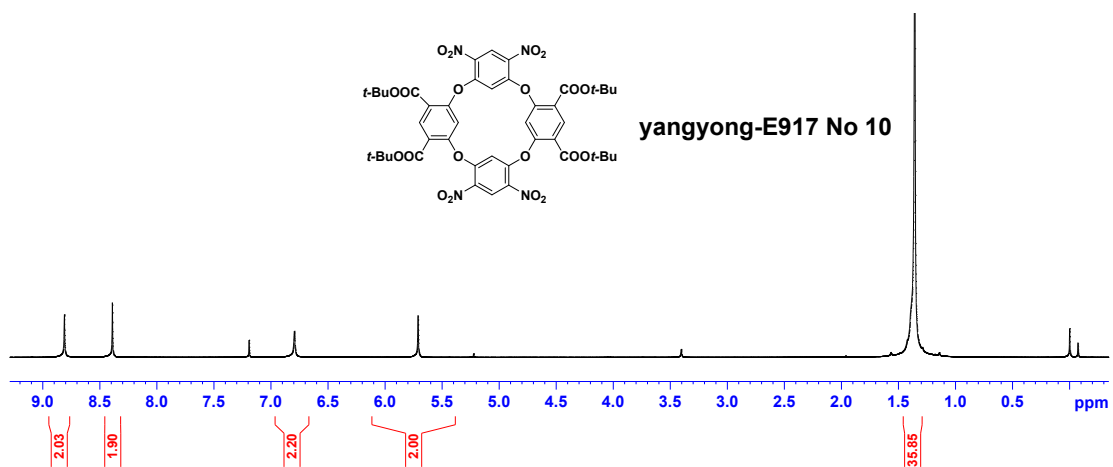
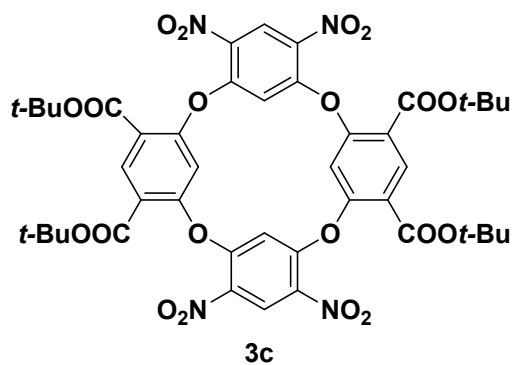
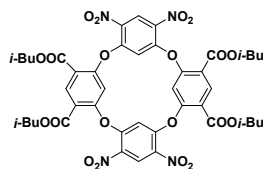
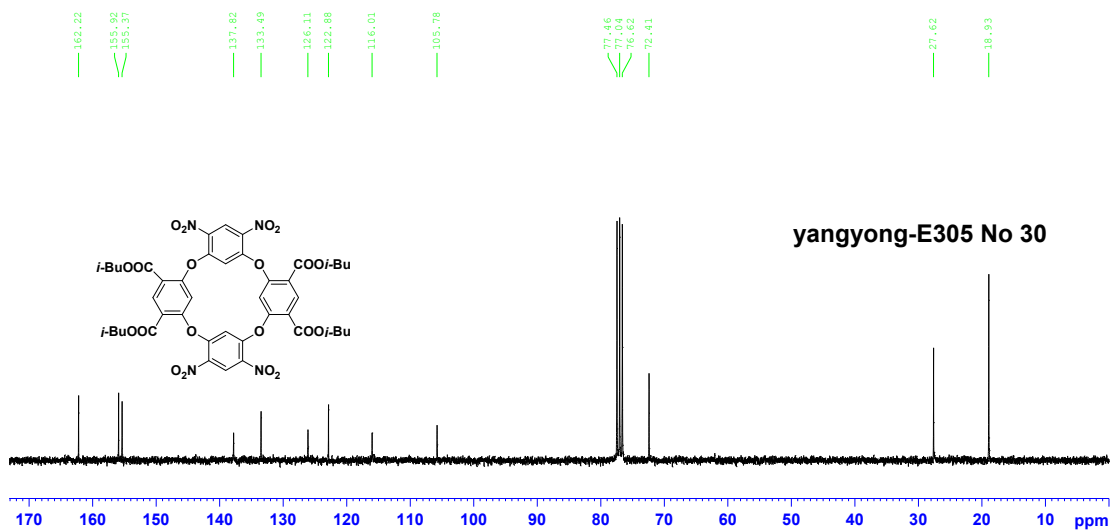
Jiao-Xia Ma, Xu Fang, Min Xue, and Yong Yang*

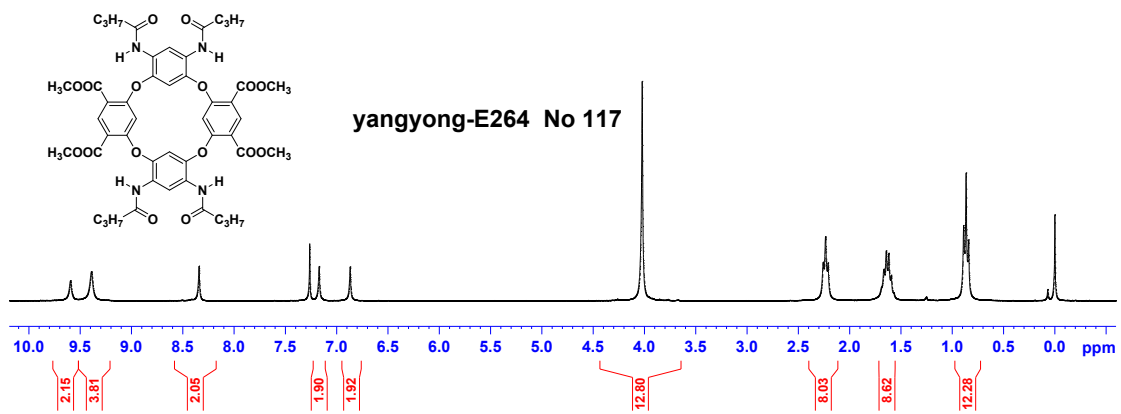
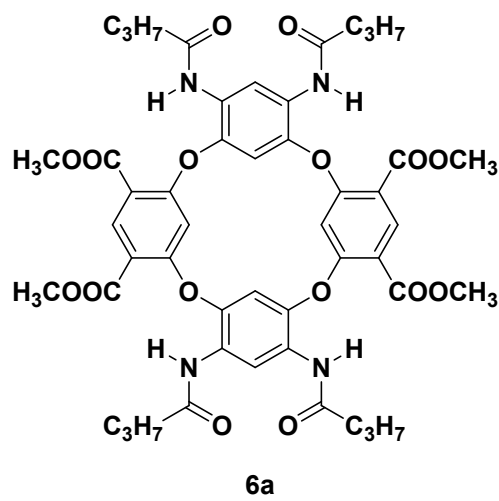
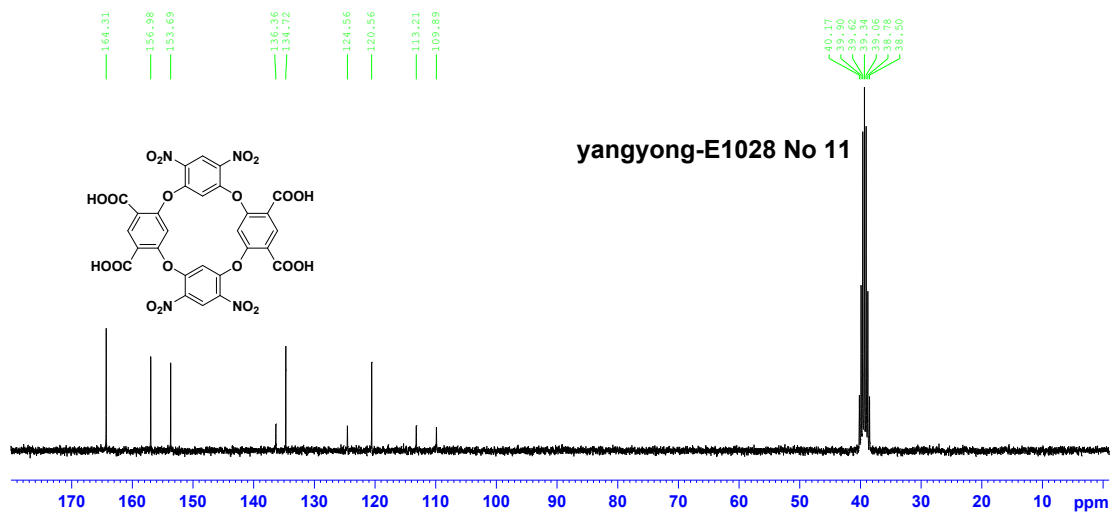
School of Sciences, Zhejiang Sci-Tech University, Hangzhou 310018, China. Email:
yangyong@zstu.edu.cn

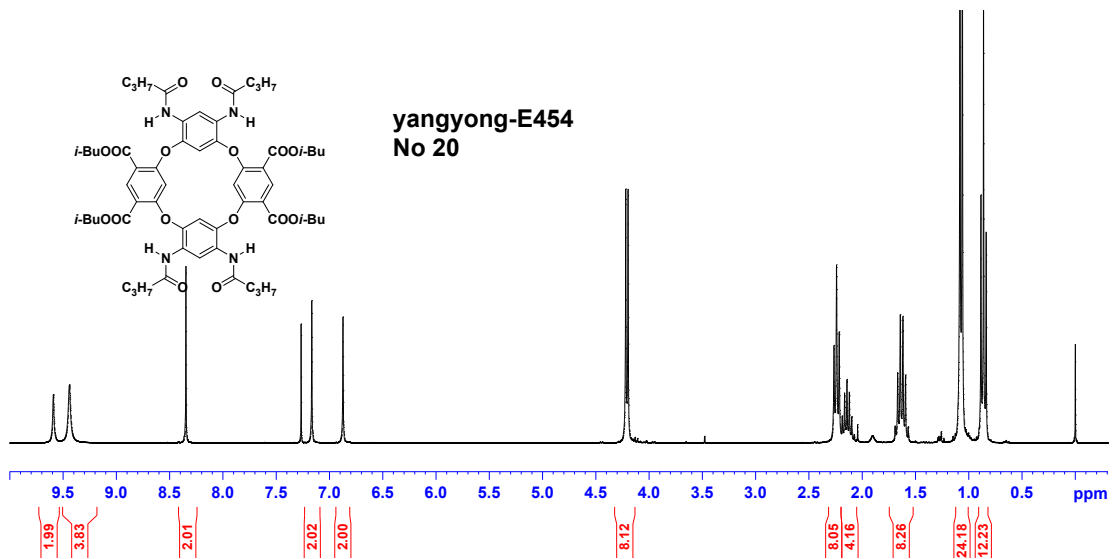
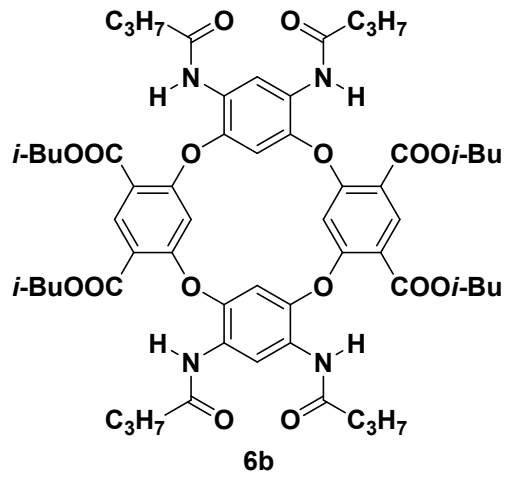
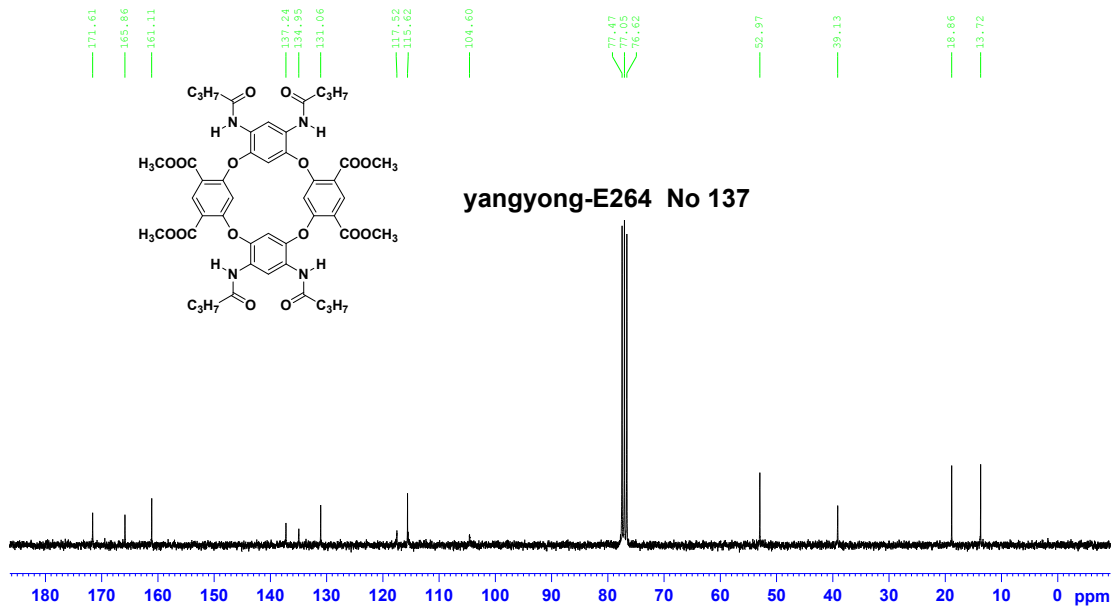


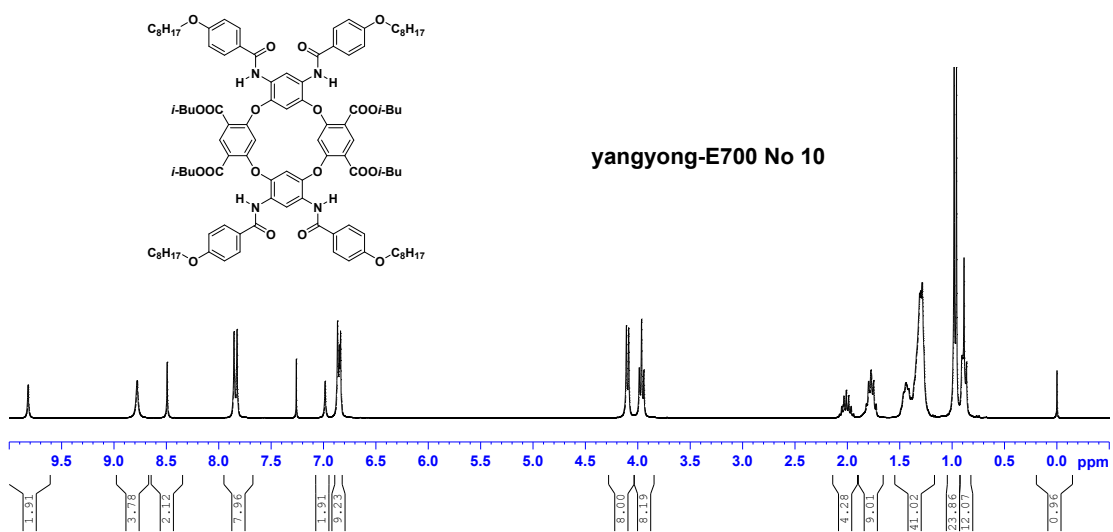
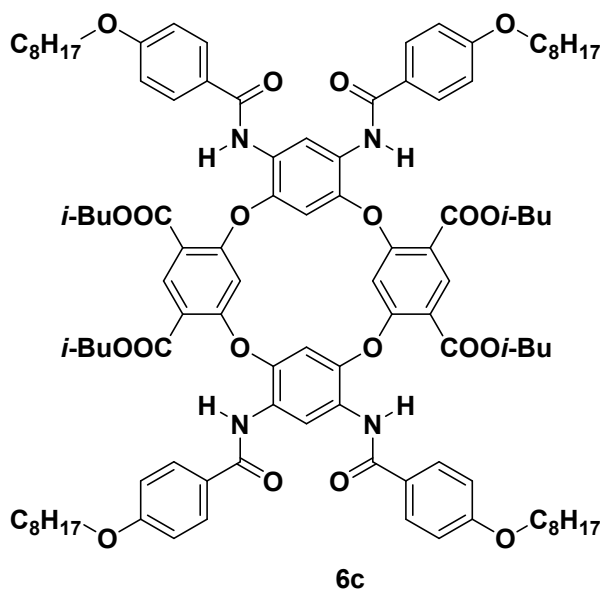
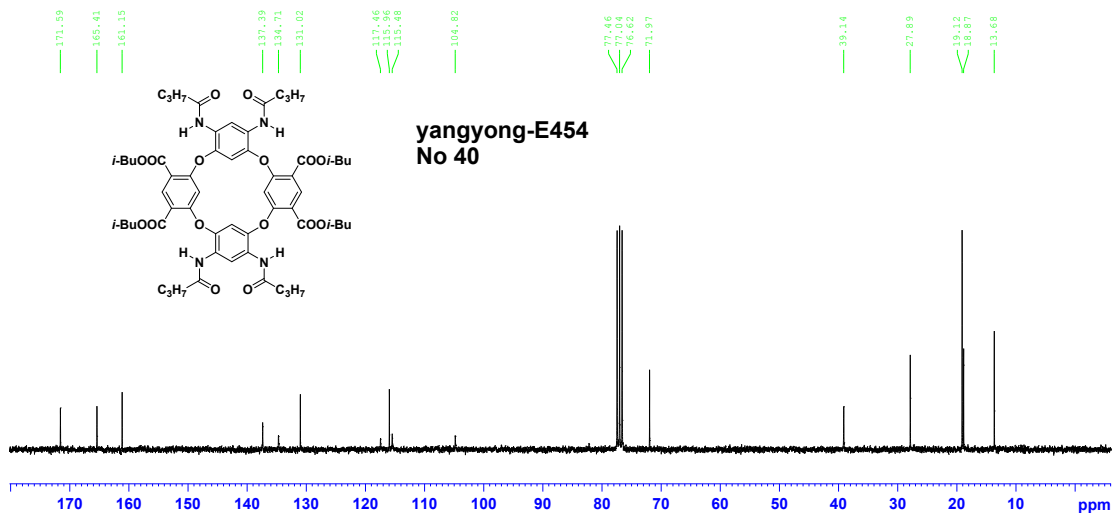


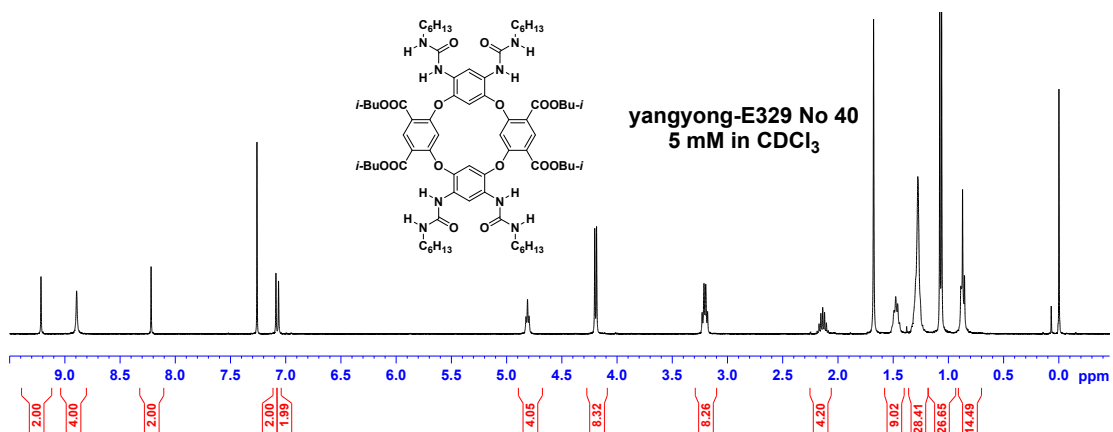
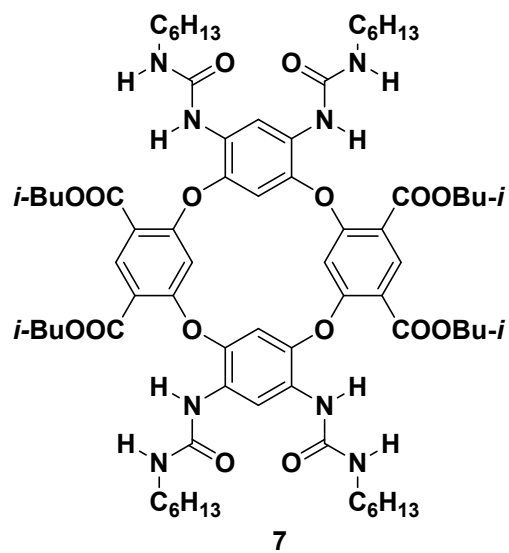
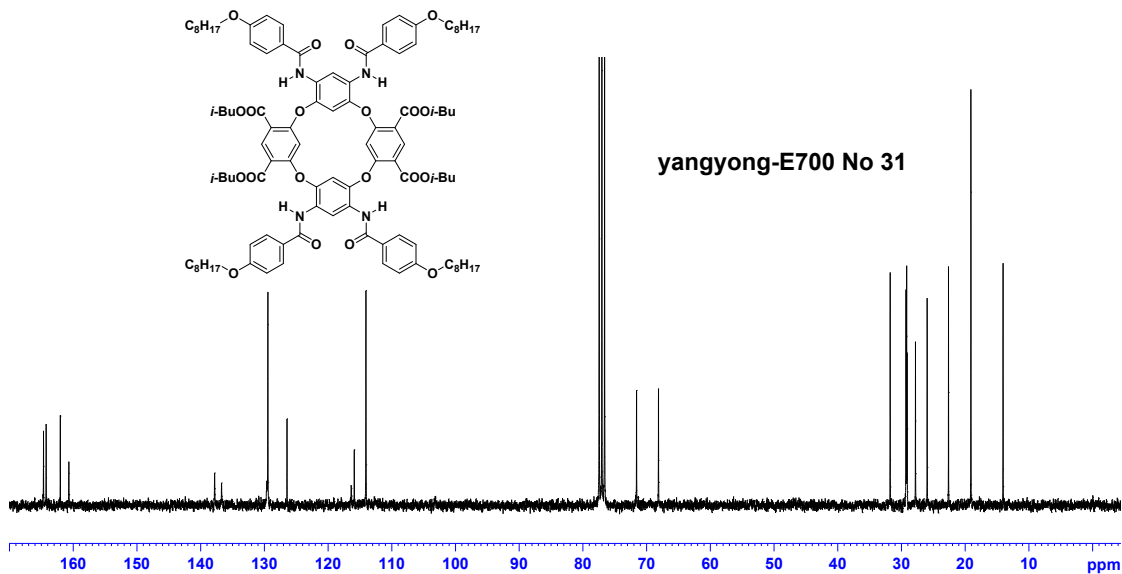


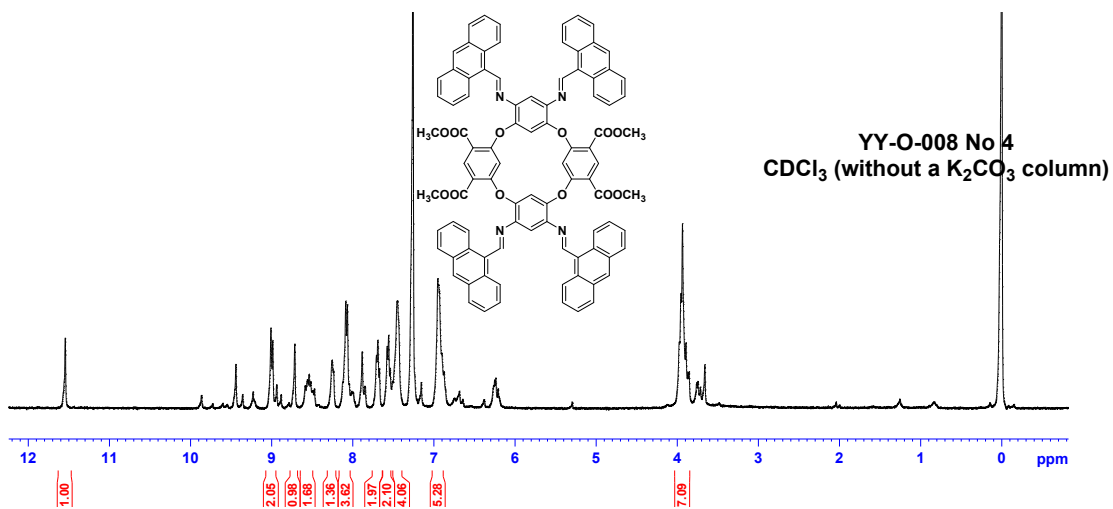
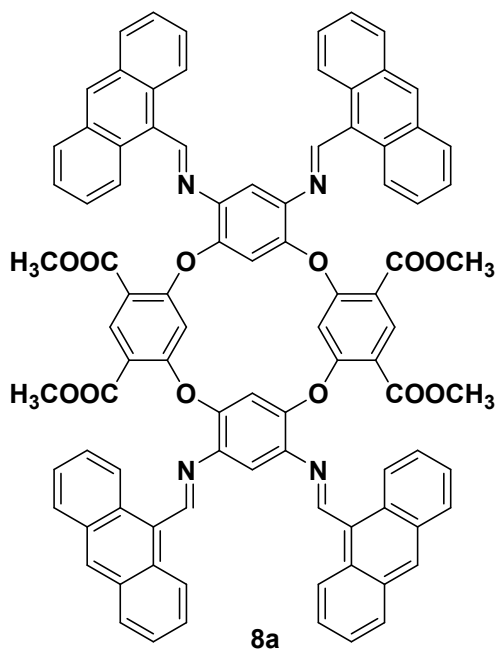
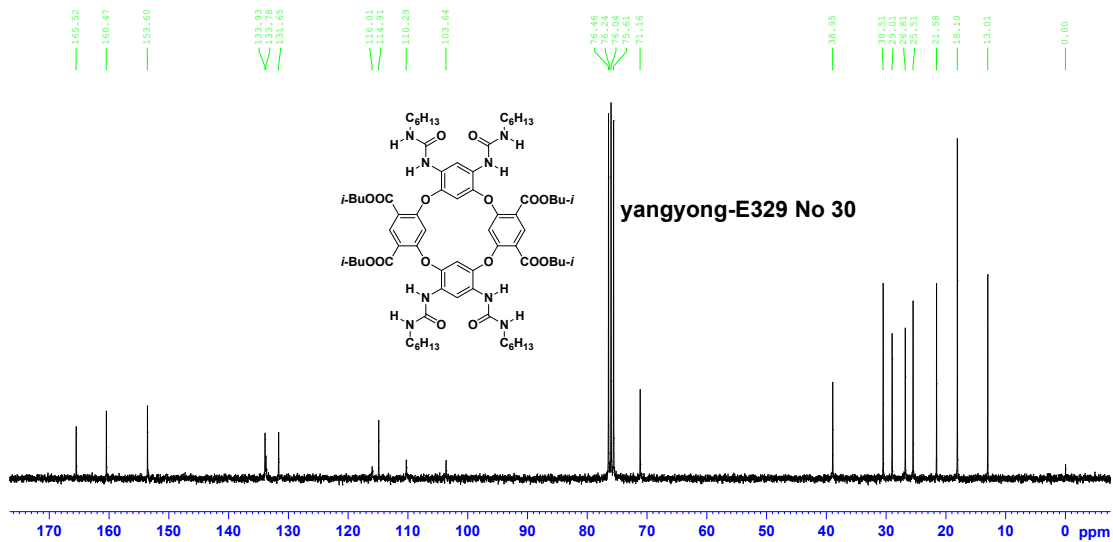


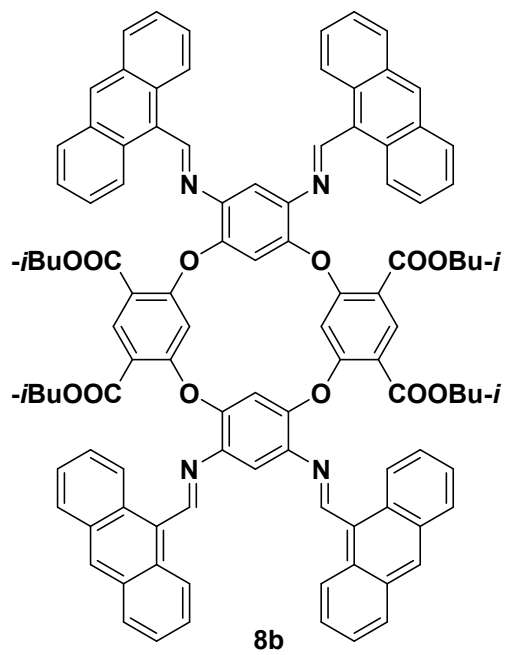
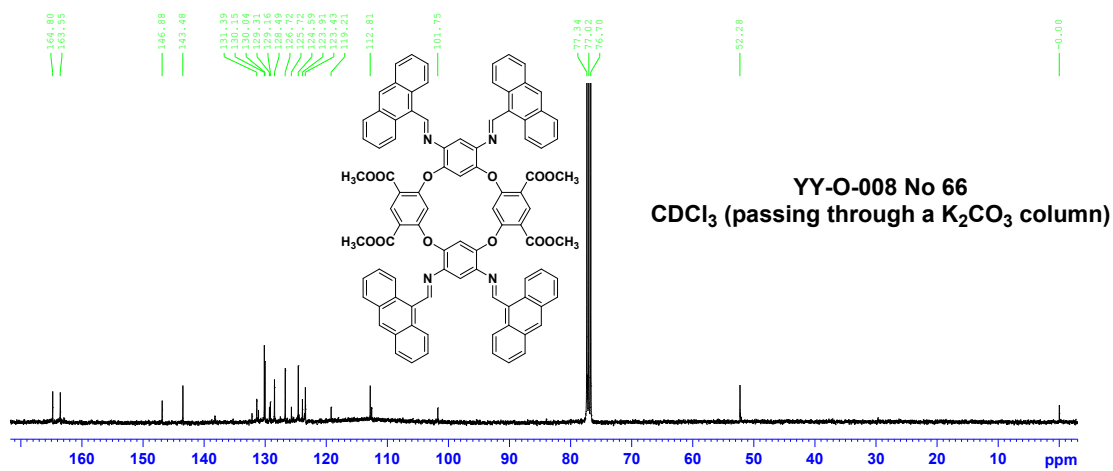
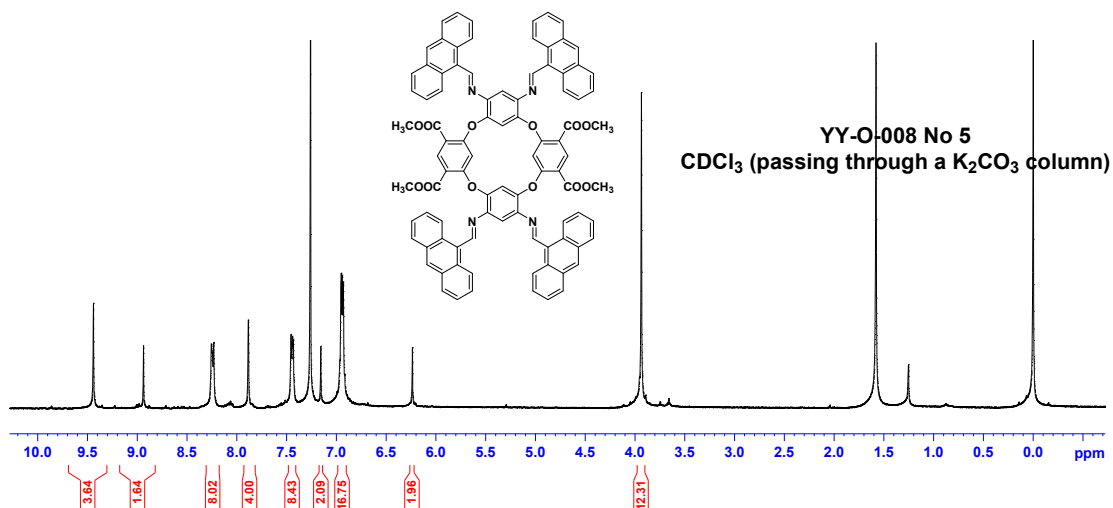


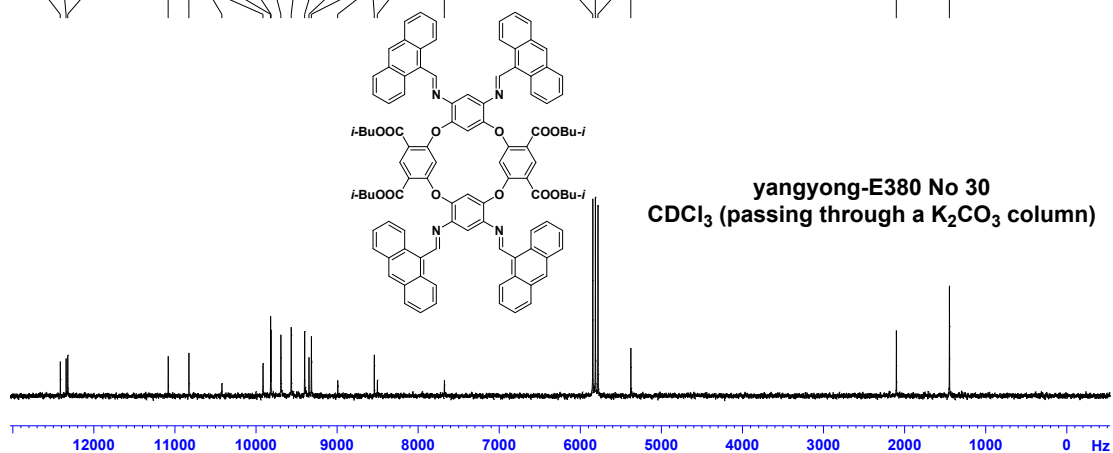
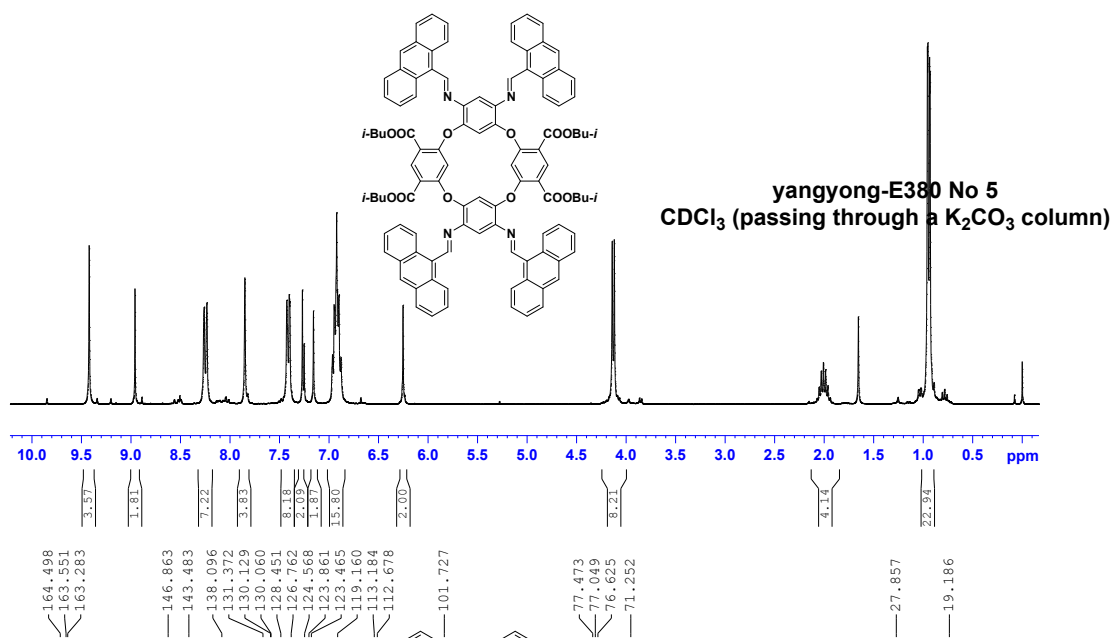
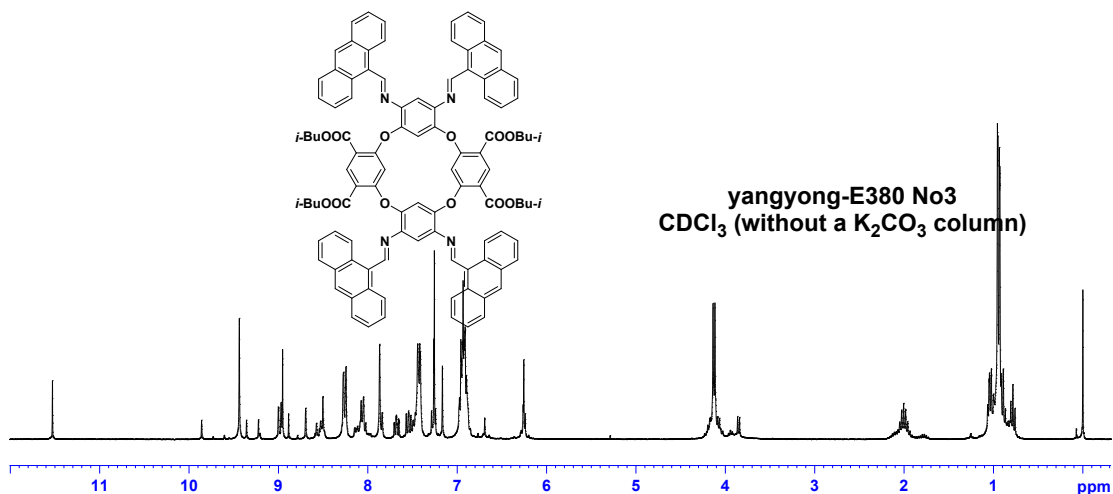


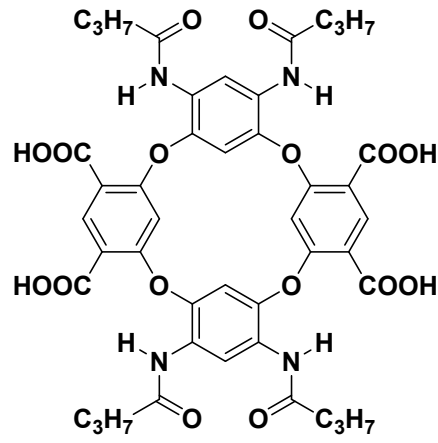




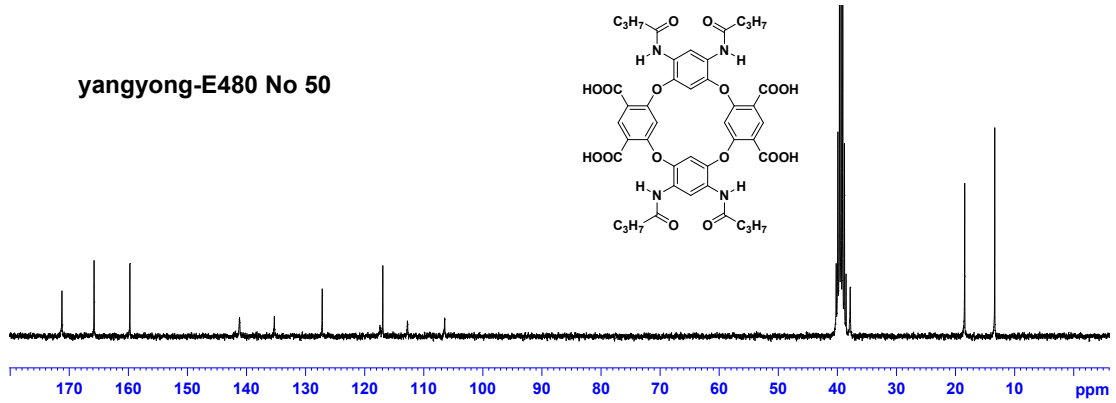
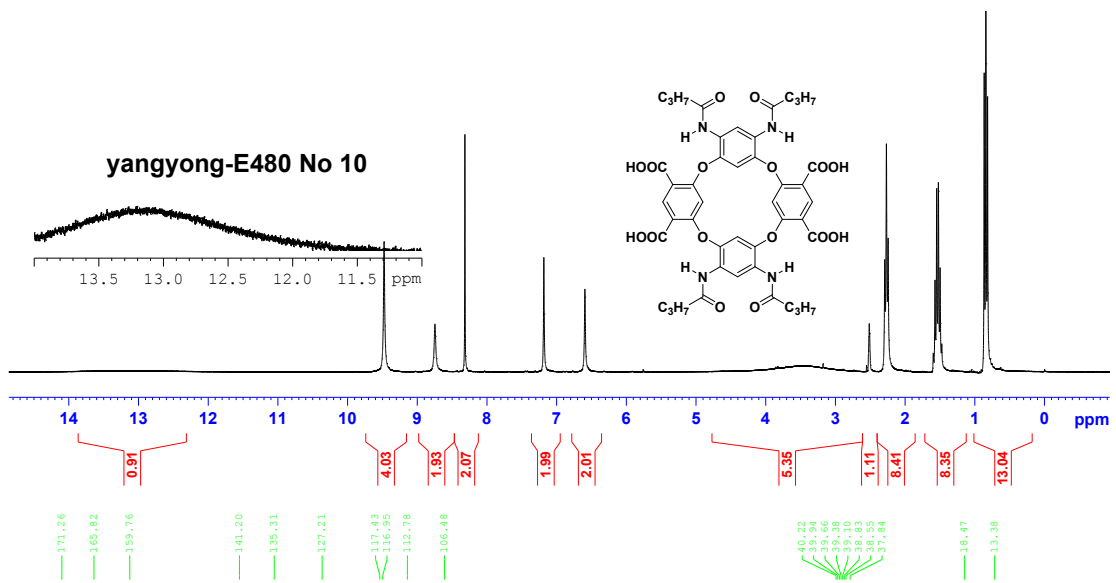


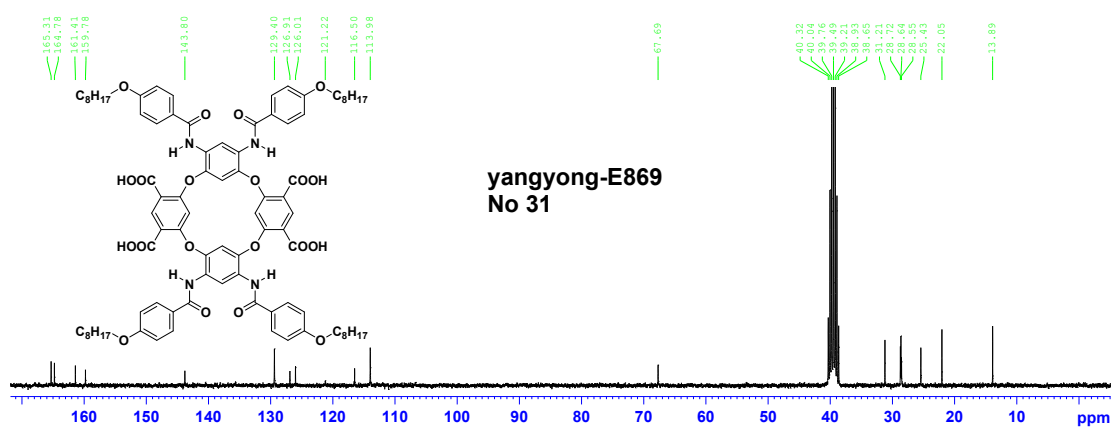
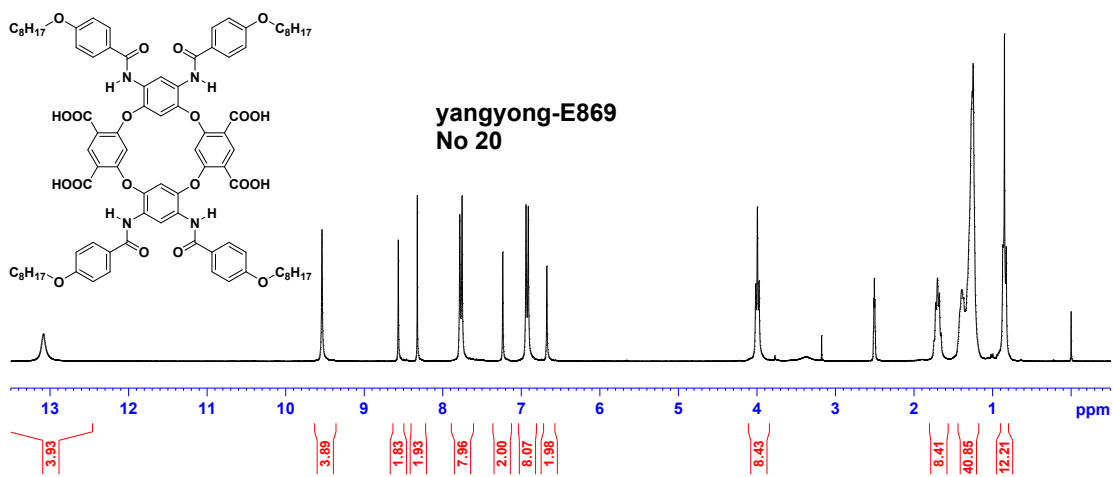
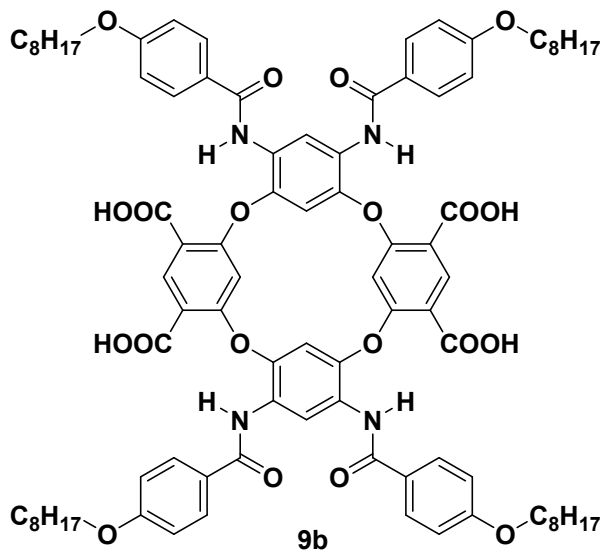


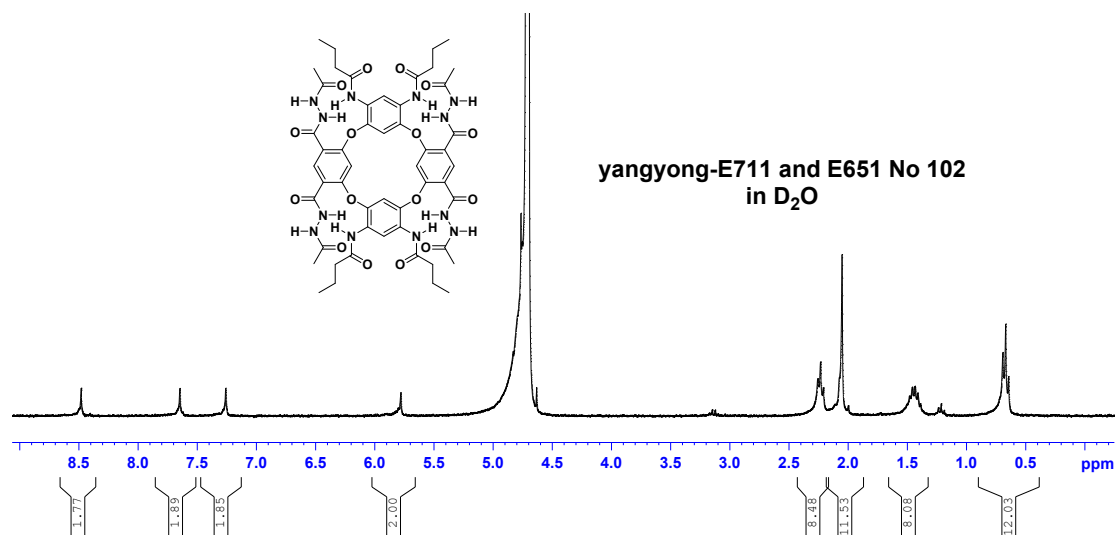
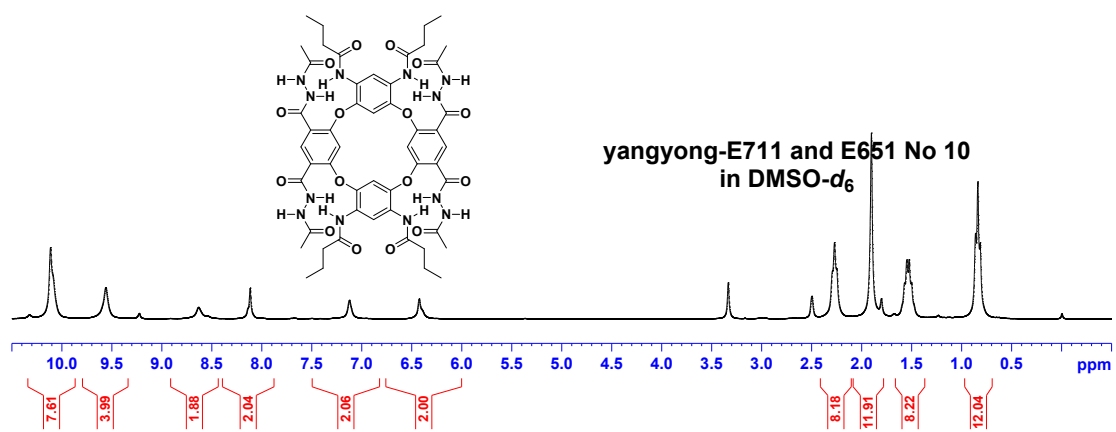
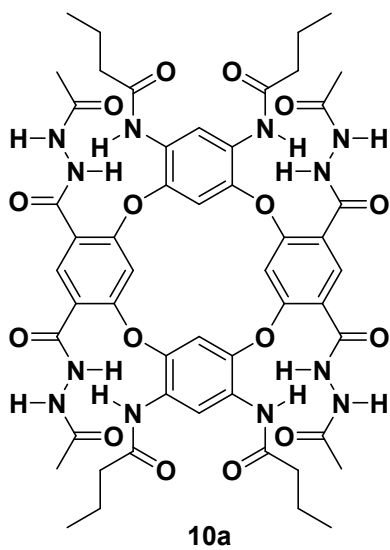


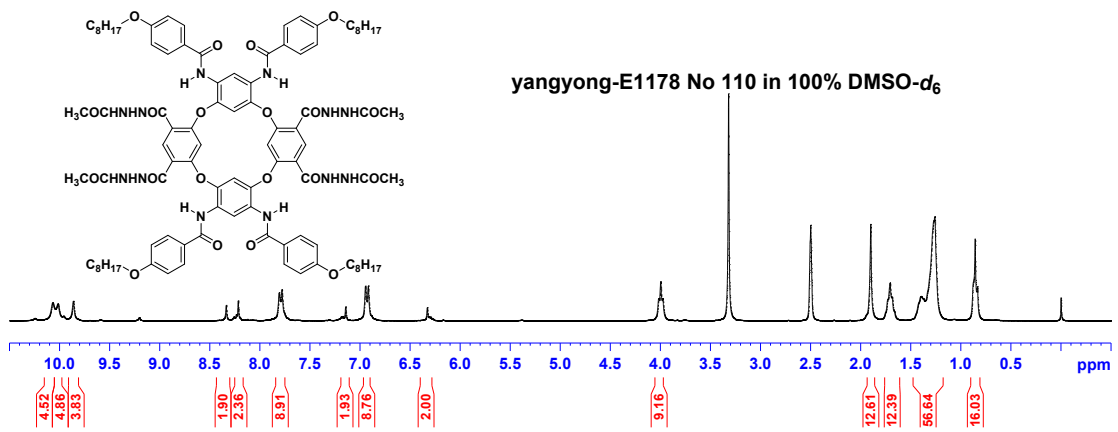
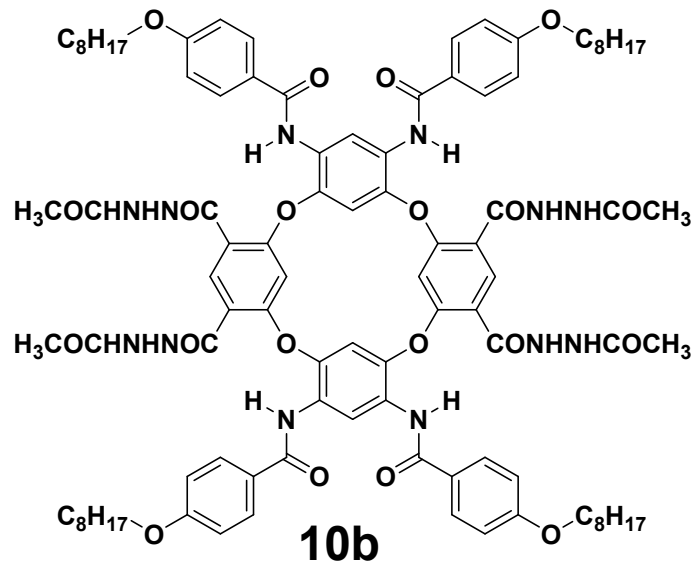
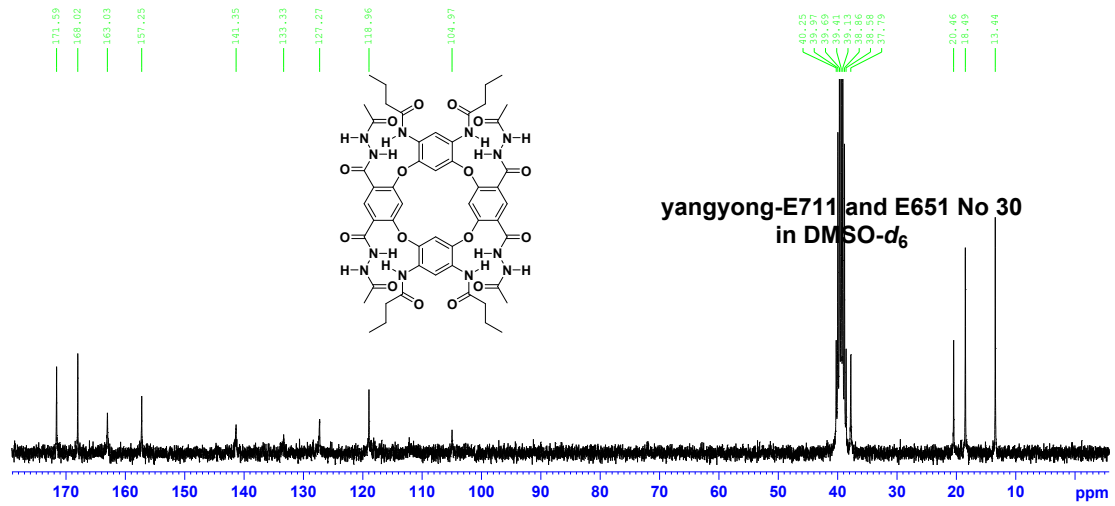


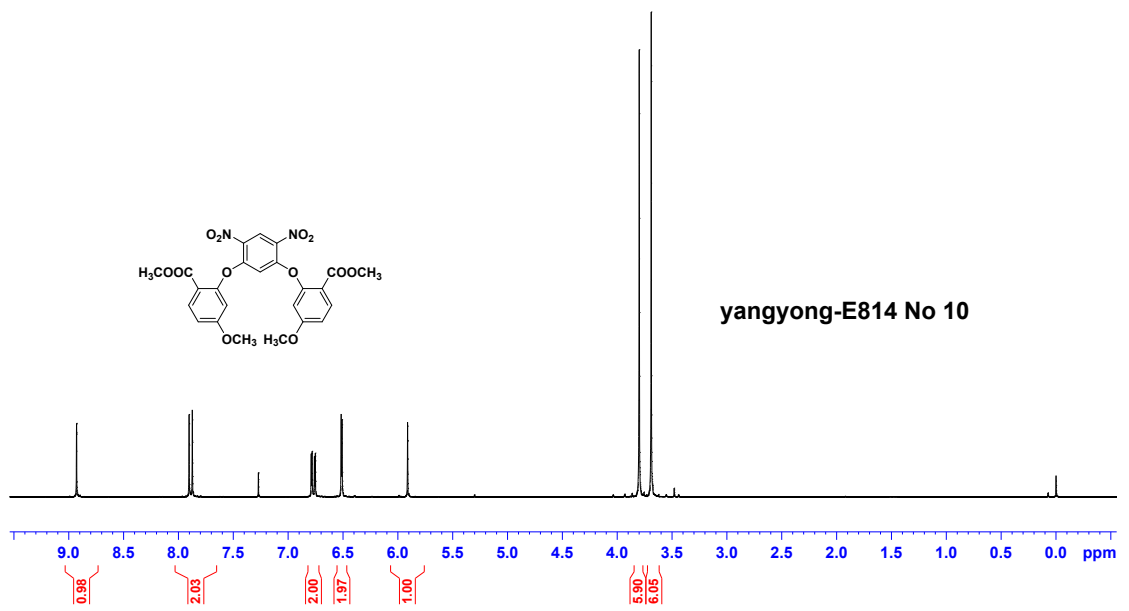
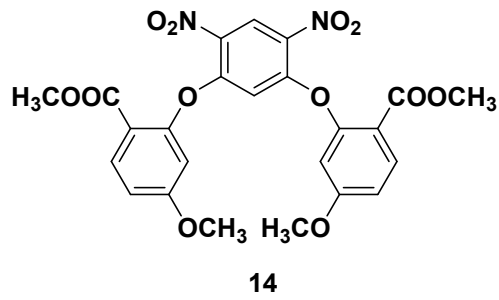
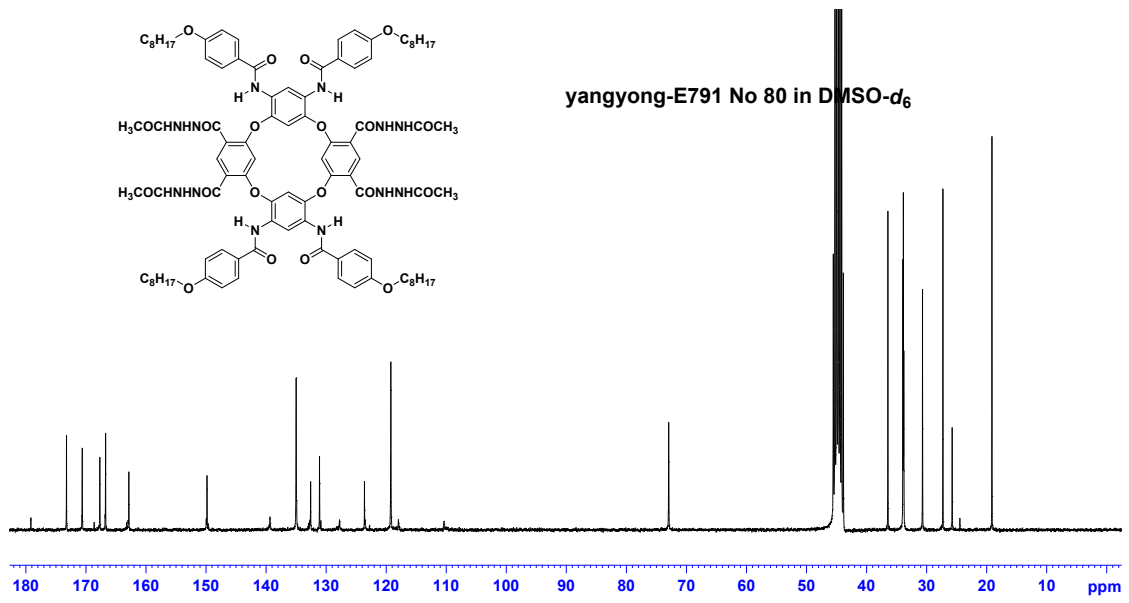
9a

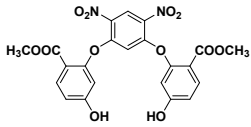
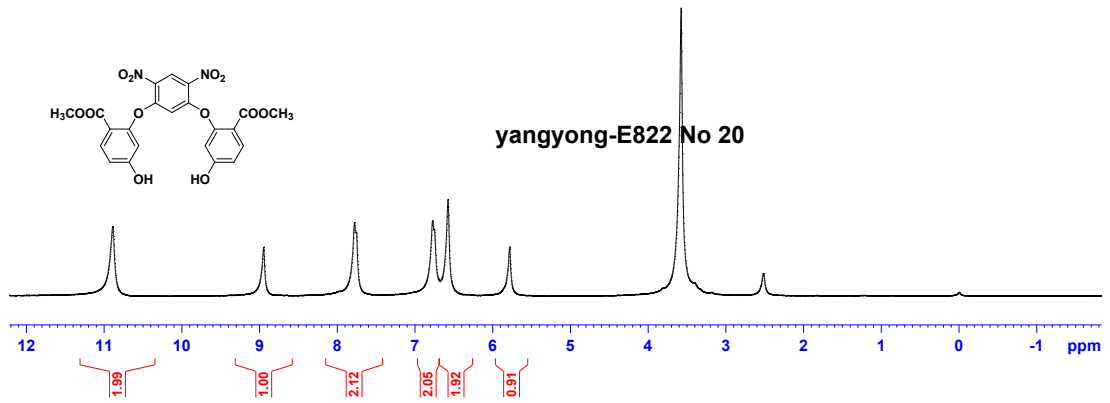
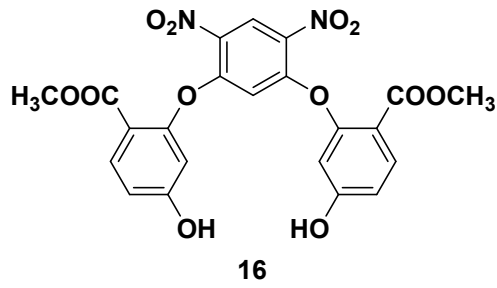
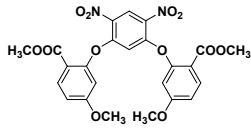
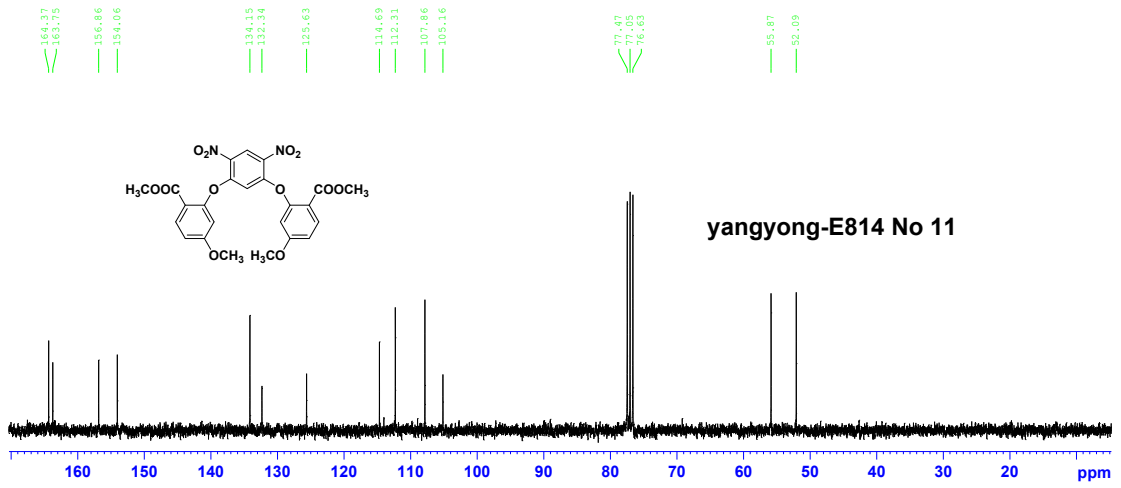


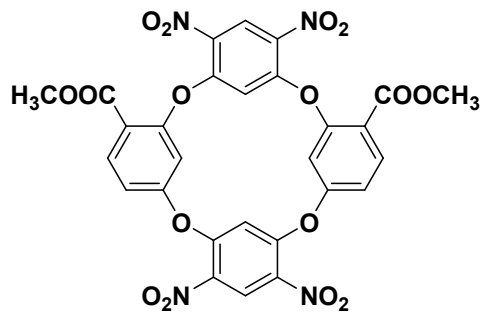
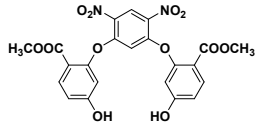
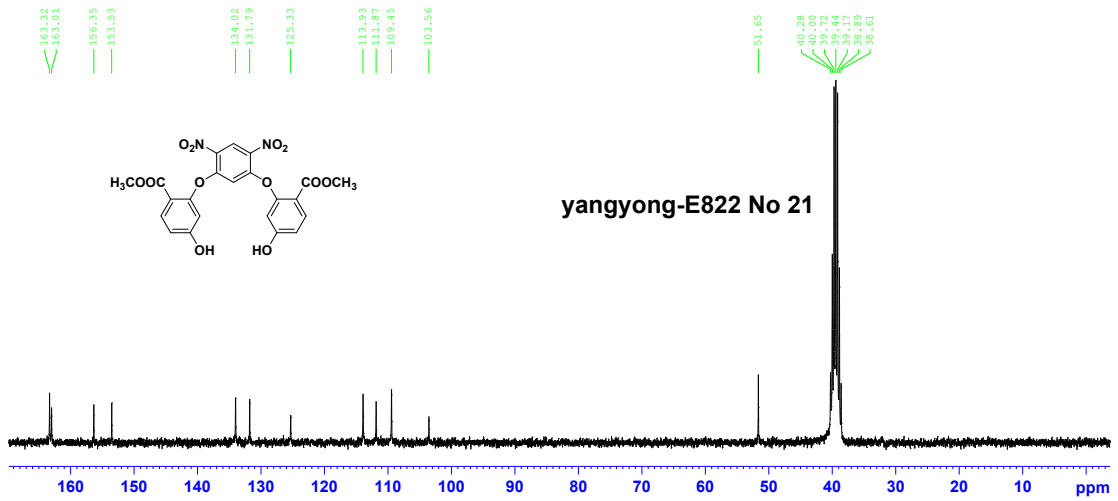




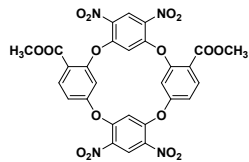
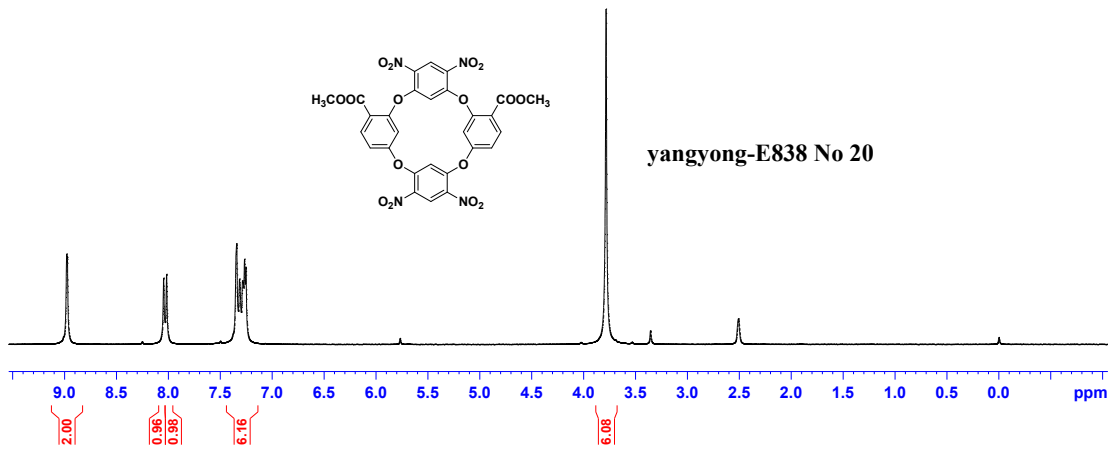


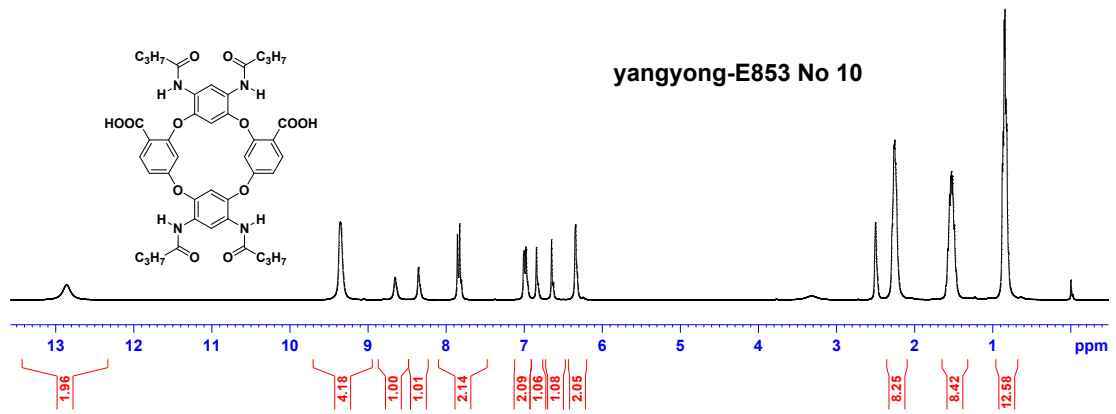
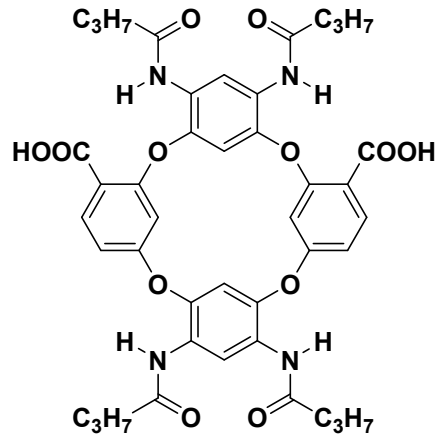
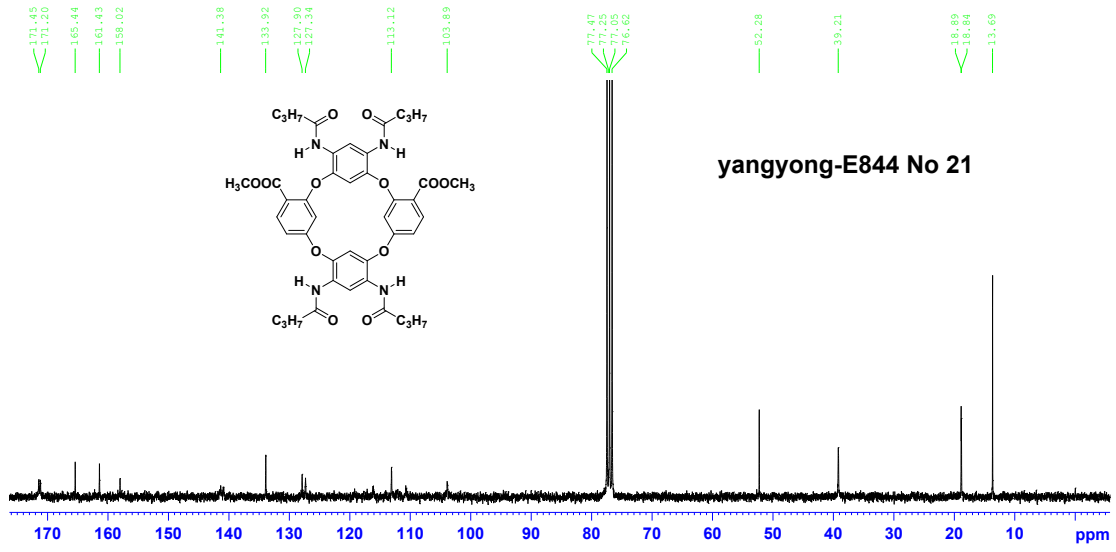






17





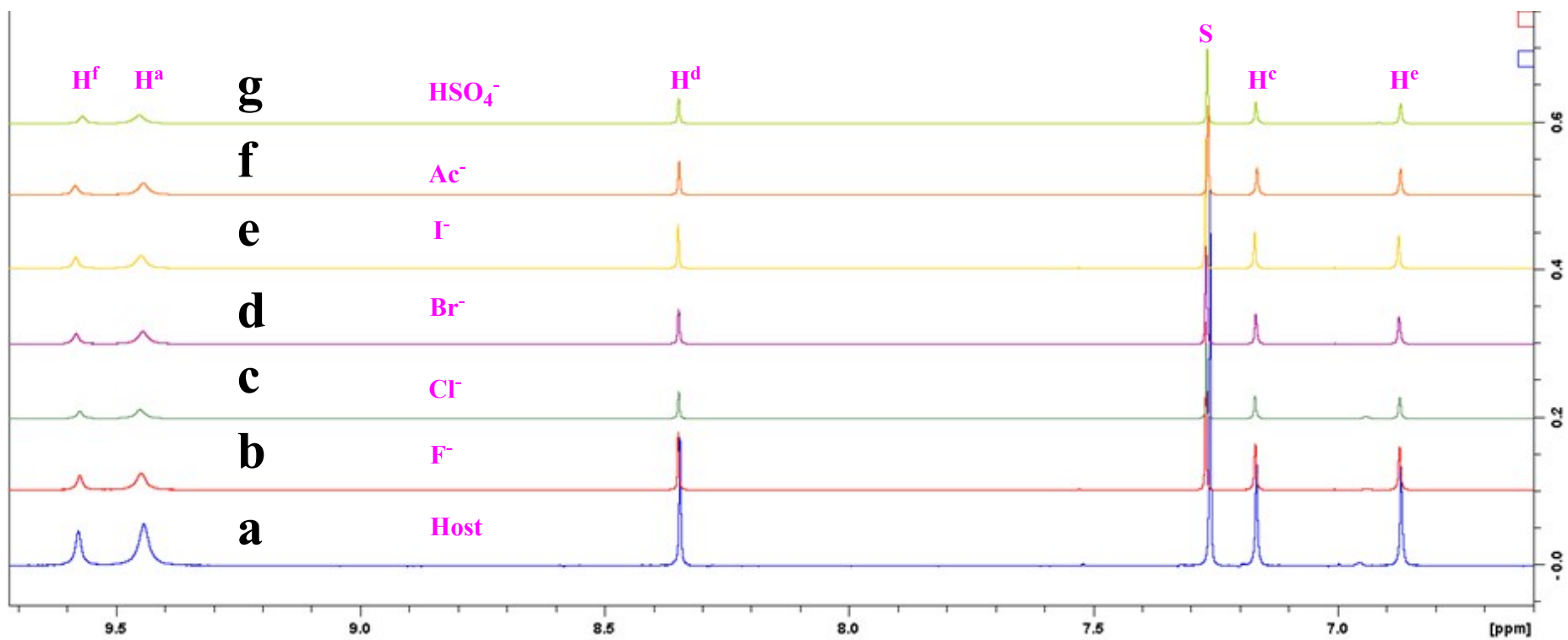


Fig. S1. Stacked partial spectra for 5 mM **6b** in CDCl₃ (a), with 15 mM Bu₄N⁺F⁻ (b), with 15 mM Bu₄N⁺Cl⁻ (c), with 15 mM Bu₄N⁺Br⁻ (d), with 15 mM Bu₄N⁺I⁻ (e), with 15 mM Bu₄N⁺Ac⁻ (f), with 15 mM Bu₄N⁺HSO₄⁻ (g), 298 K, 400 MHz.

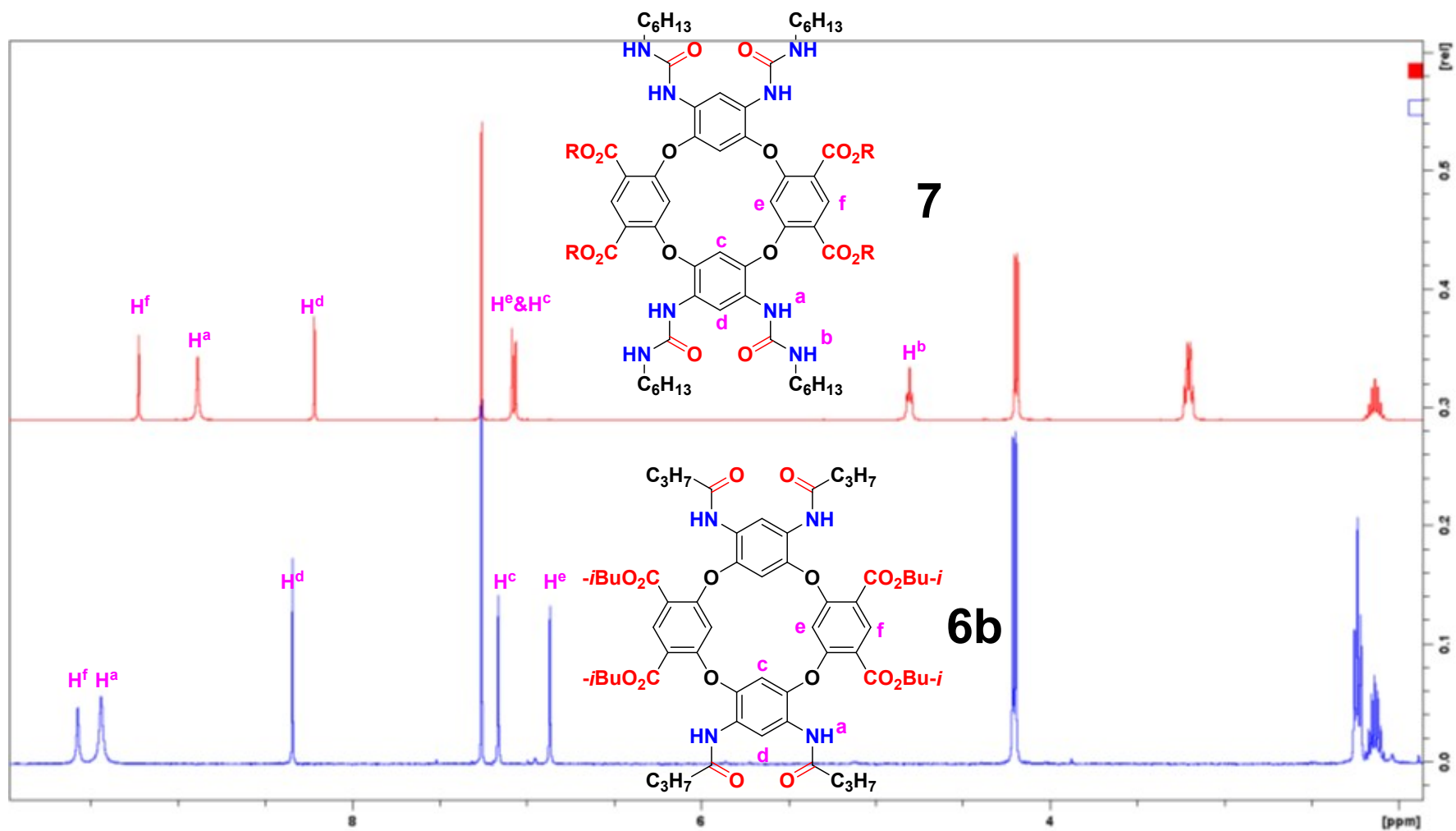


Fig. S2. Stacked partial spectra for 5 mM **6b** (bottom) and 5 mM **7** (up), CDCl₃, 298 K, 400 MHz.

Determination of association constant (K_a) of Tetraureido Oxacalix[4]arene **7** and the anion guests F^- , Cl^- , Br^- , I^- , Ac^- , and HSO_4^- , from UV-vis titration data was based on the following equation.^{S1-S2}



$$K_a = \frac{[HG]}{[H][G]}$$

$$[H] = [H]_0 - [HG]$$

$$[G] = [G]_0 - [HG]$$

$$[HG] = \frac{[G]_0 + [H]_0 + \frac{1}{K_a} - \sqrt{([G]_0 + [H]_0 + \frac{1}{K_a})^2 - 4[G]_0[H]_0}}{2}$$

$$A_{obs} = \varepsilon_1[H] + \varepsilon_2[HG]$$

$$= \varepsilon_1([H]_0 - [HG]) + \varepsilon_2[HG]$$

$$= \varepsilon_1[H]_0 + (\varepsilon_2 - \varepsilon_1)[HG] \quad A_0 = \varepsilon_1[H]_0$$

$$A_{obs} - A_0 = (\varepsilon_2 - \varepsilon_1)[HG]$$

$$\Delta A = A_{obs} - A_0 \quad C = \varepsilon_2 - \varepsilon_1$$

$$\Delta A = C \frac{[G]_0 + [H]_0 + \frac{1}{K_a} - \sqrt{([G]_0 + [H]_0 + \frac{1}{K_a})^2 - 4[G]_0[H]_0}}{2}$$

(Eq. S1)

$[H]_0$: the initial concentration of Host

$[H]$: the concentration of free Host

$[G]_0$: the initial concentration of Guest

$[G]$: the concentration of free Guest

$[HG]$: the concentration of Host-Guest complex

K_a : association constant

ε_1 : molar absorption coefficient of Host

ε_2 : molar absorption coefficient of Host-Guest complex HG

A_0 : the initial absorption value of Host

A_{obs} : absorption value measured for each titration

ΔA : changes for absorption value

C : constant

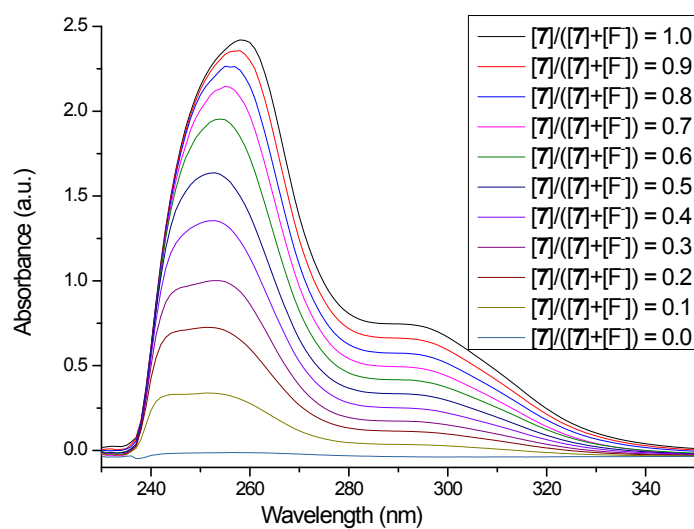


Fig. S3. UV-vis spectra of mixtures of host **7** and guest $\text{Bu}_4\text{N}^+\text{F}^-$ with different ratios in CHCl_3 , with the total concentration fixed at 5×10^{-5} M.

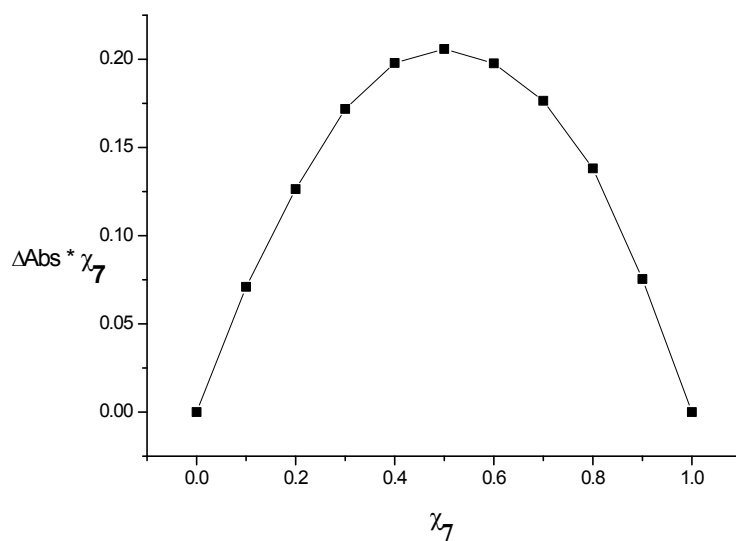


Fig. S4. Job-plot for the complex between host **7** and guest $\text{Bu}_4\text{N}^+\text{F}^-$ in CHCl_3 using UV-vis absorption values at $\lambda = 290$ nm, showing a 1:1 stoichiometry.

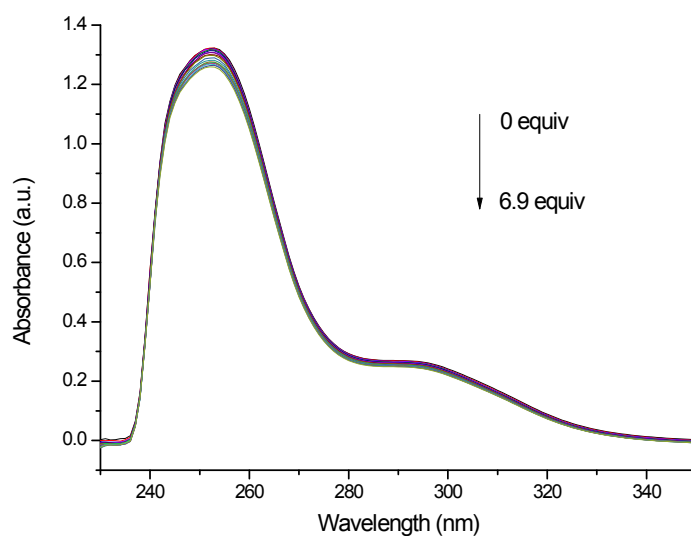


Fig. S5. Titration curves of host **7** (fixed at 2×10^{-5} M in CHCl_3) with 0-6.9 equivalents of guest $\text{Bu}_4\text{N}^+\text{F}^-$, 298 K.

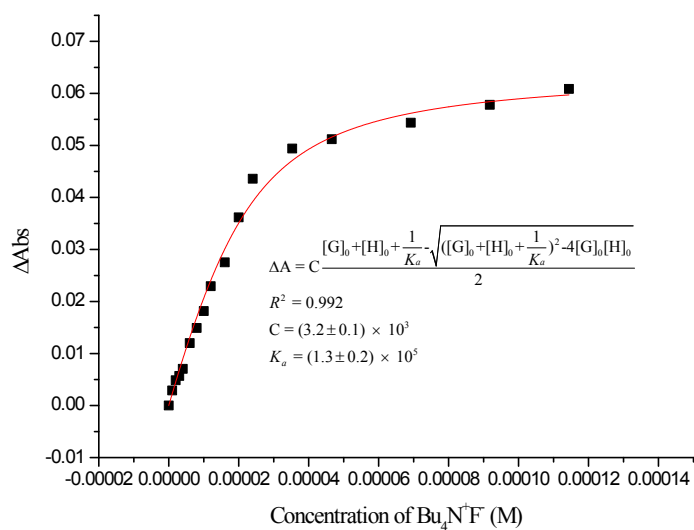


Fig. S6. Plot of the absorption intensity changes at $\lambda = 254$ nm vs the guest concentration. The red line was obtained from non-linear curve-fitting using Eq. S1, yielding an association constant $K_a = (1.3 \pm 0.2) \times 10^5 \text{ M}^{-1}$.

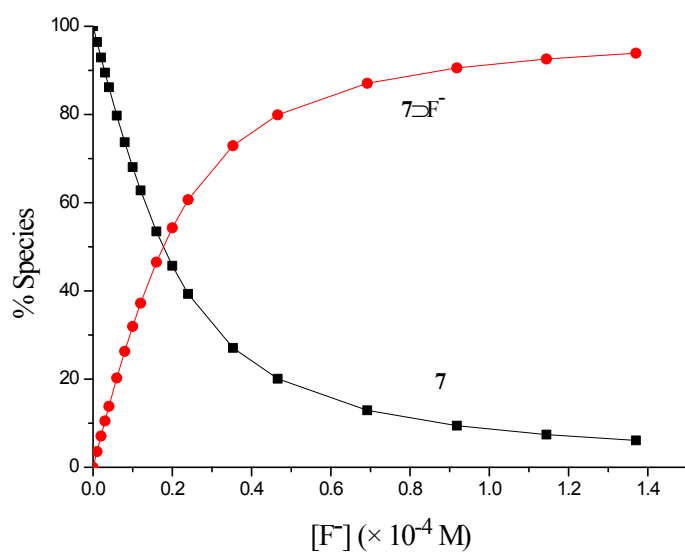


Fig. S7. Distribution diagram between **7** and **7-F⁻** during the spectrophotometric titration, calculated using UV-vis titration absorption data at $\lambda = 254$ nm.

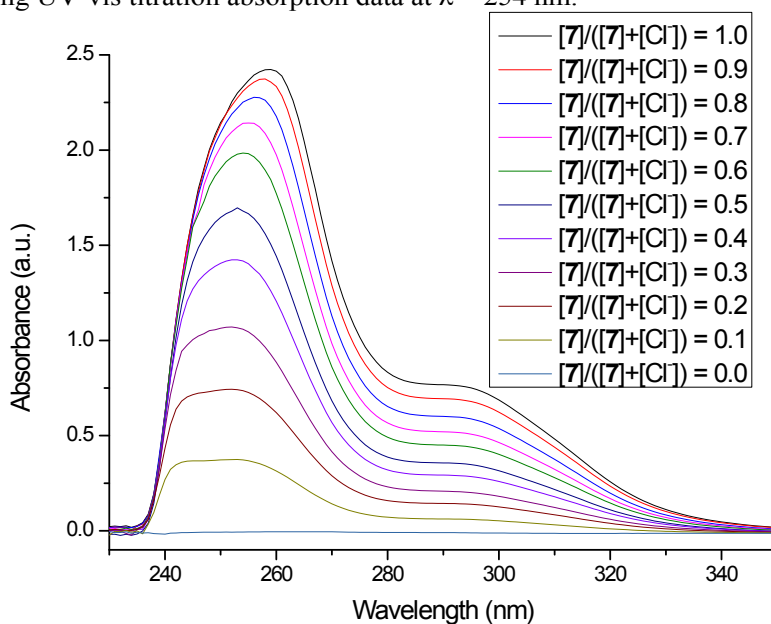


Fig. S8. UV-vis spectra of mixtures of host **7** and guest $\text{Bu}_4\text{N}^+\text{Cl}^-$ with different ratios in CHCl_3 , with the total concentration fixed at 5×10^{-5} M.

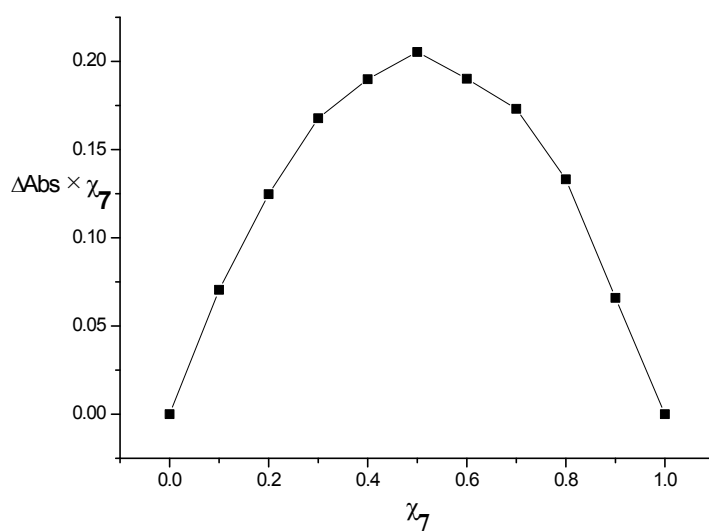


Fig. S9. Job-plot for the complex between host **7** and guest $\text{Bu}_4\text{N}^+\text{Cl}^-$ in CHCl_3 using UV-vis absorption values at $\lambda = 290$ nm, showing a 1:1 stoichiometry.

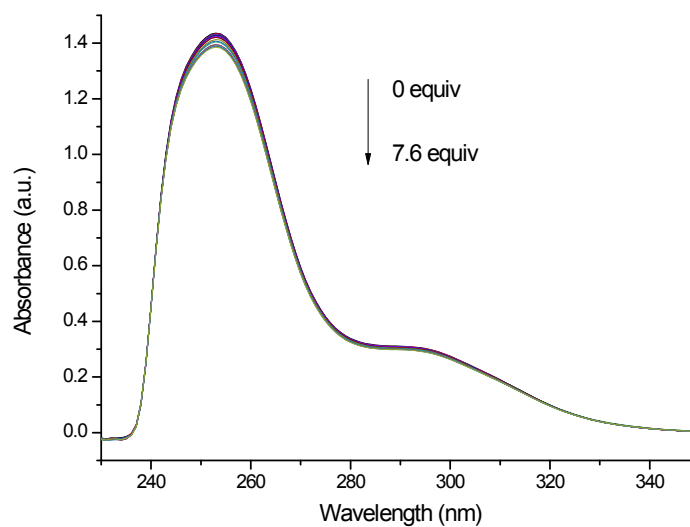


Fig. S10. Titration curves of host **7** (fixed at 2×10^{-5} M in CHCl_3) with 0-7.6 equivalents of guest $\text{Bu}_4\text{N}^+\text{Cl}^-$, 298 K.

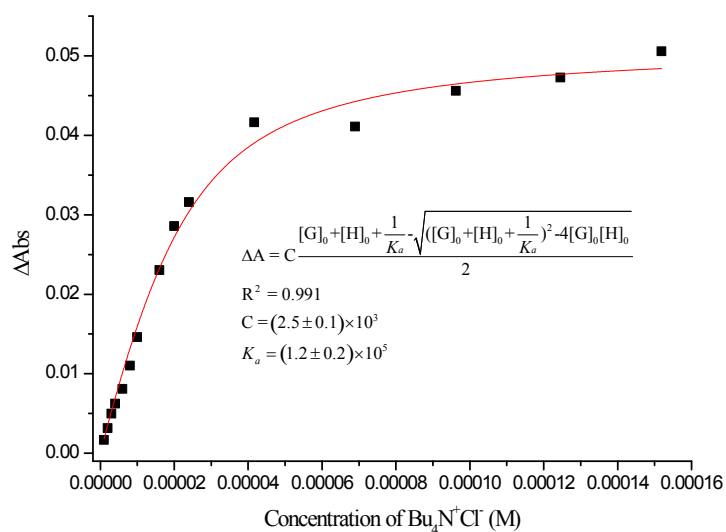


Fig. S11. Plot of the absorption intensity changes at $\lambda = 253$ nm vs the guest concentration. The red line was obtained from non-linear curve-fitting using Eq. S1, yielding an association constant $K_a = (1.2 \pm 0.2) \times 10^5 \text{ M}^{-1}$.

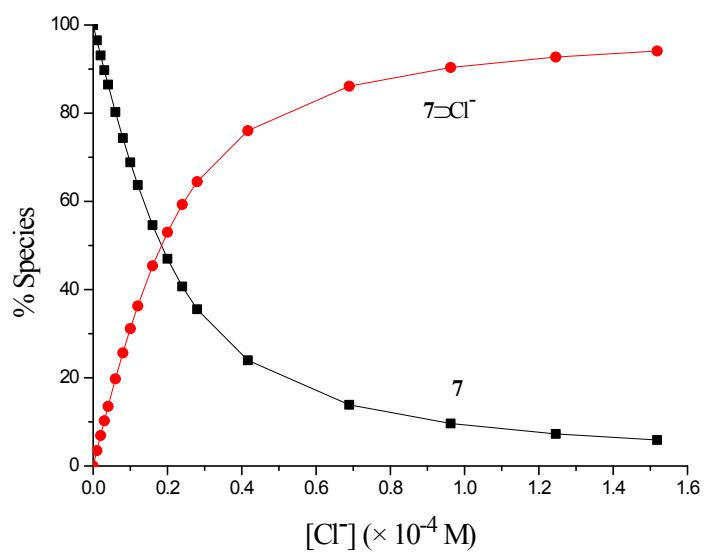


Fig. S12. Distribution diagram between **7** and **7=Cl⁻** during the spectrophotometric titration, calculated using UV-vis titration absorption data at $\lambda = 253$ nm.

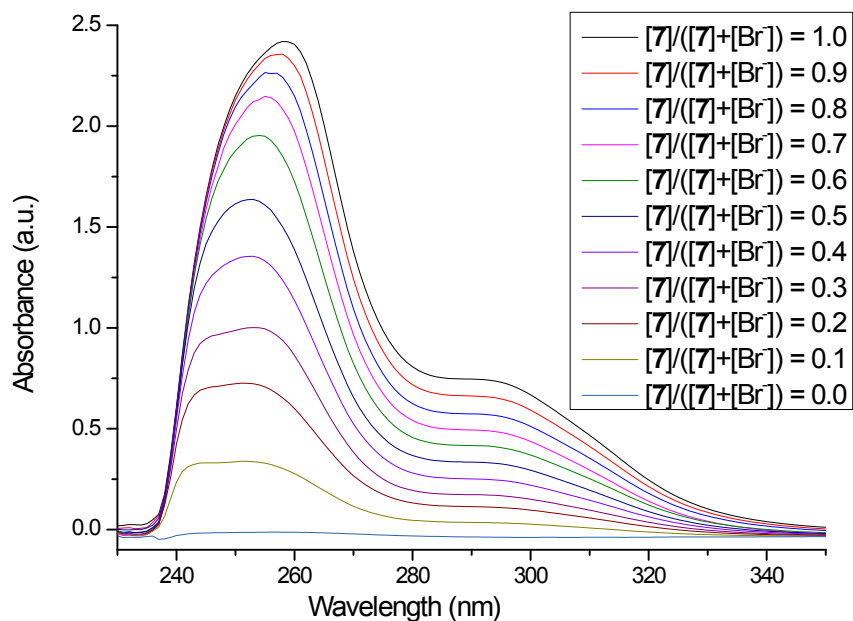


Fig. S13. UV-vis spectra of mixtures of host 7 and guest $\text{Bu}_4\text{N}^+\text{Br}^-$ with different ratios in CHCl_3 , with the total concentration fixed at 5×10^{-5} M.

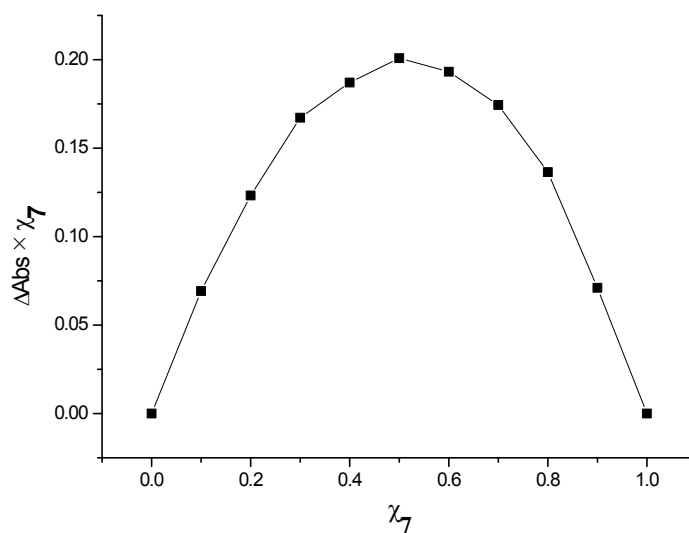


Fig. S14. Job-plot for the complex between host 7 and guest $\text{Bu}_4\text{N}^+\text{Br}^-$ in CHCl_3 using UV-vis absorption value at $\lambda = 290$ nm, showing a 1:1 stoichiometry.

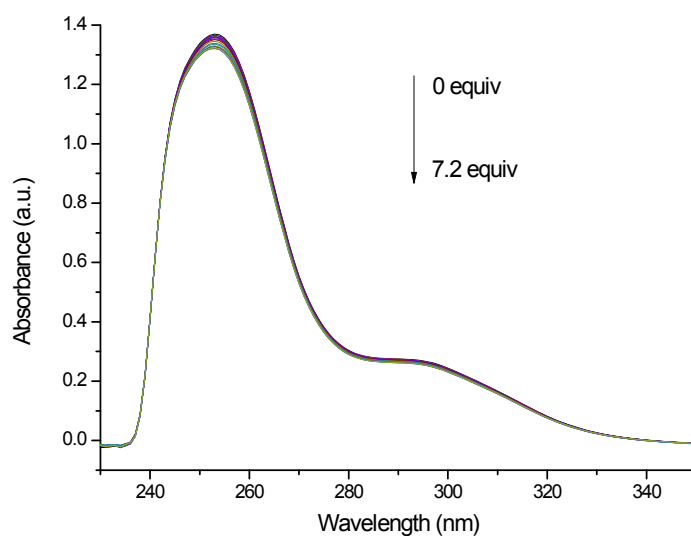


Fig. S15. Titration curves of host **7** (fixed at 2×10^{-5} M in CHCl_3) with 0-7.2 equivalents of guest $\text{Bu}_4\text{N}^+\text{Br}^-$, 298 K.

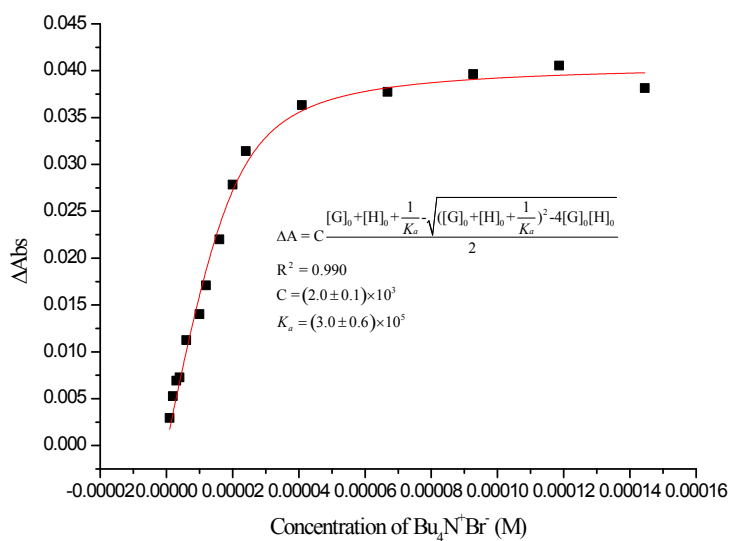


Fig. S16. Plot of the absorption intensity changes at $\lambda = 250$ nm vs the guest concentration. The red line was obtained from non-linear curve-fitting using Eq. S1, yielding an association constant $K_a = (3.0 \pm 0.6) \times 10^5 \text{ M}^{-1}$.

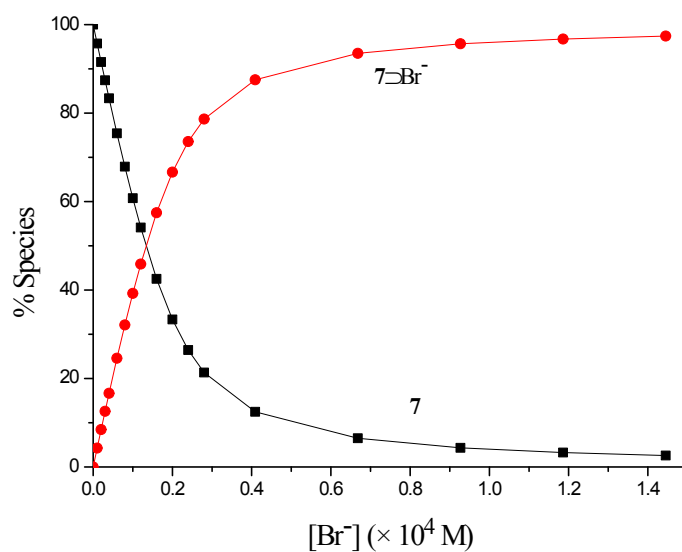


Fig. S17. Distribution diagram between **7** and **7⊃Br⁻** during the spectrophotometric titration, calculated using UV-vis titration absorption data at $\lambda = 250$ nm.

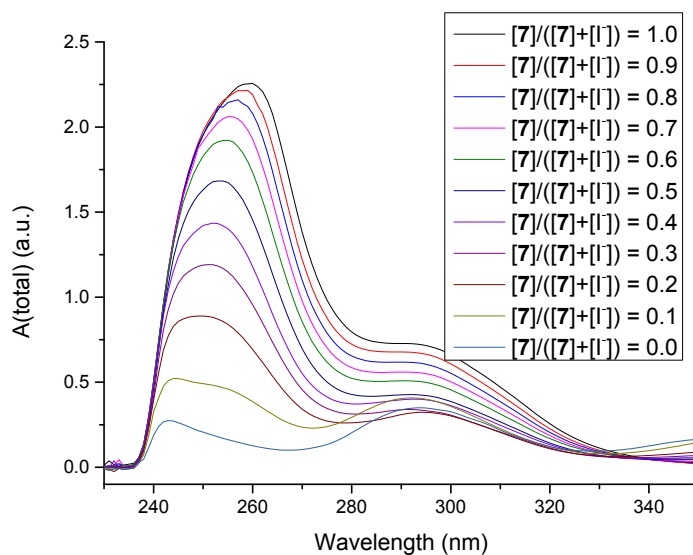


Fig. S18. UV-vis spectra of a mixture of host **7** and guest $\text{Bu}_4\text{N}^+\text{I}^-$ with different ratios in CHCl_3 , with the total concentration fixed at 5×10^{-5} M.

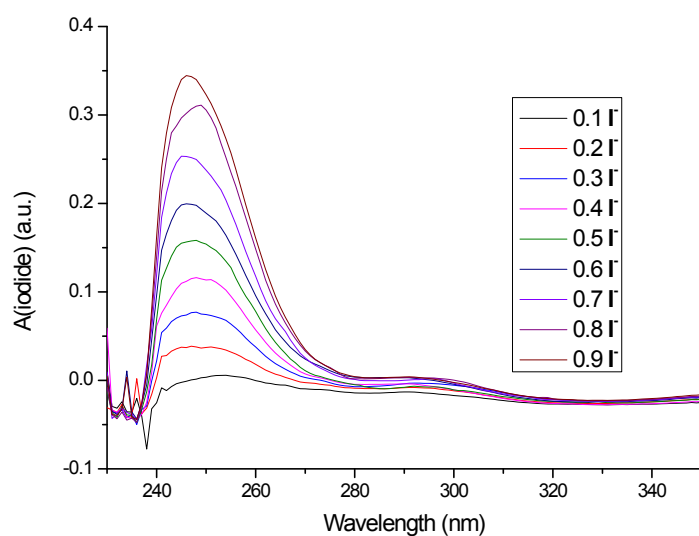


Fig. S19. UV-vis spectra of guest $\text{Bu}_4\text{N}^+\text{I}^-$ with the same concentrations in the above measurements.

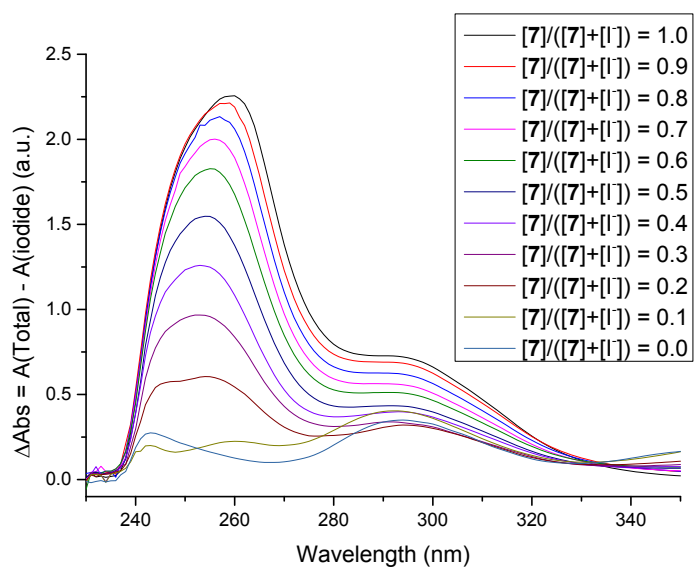


Fig. S20. UV-vis spectra, after deduction of I^- absorbance.

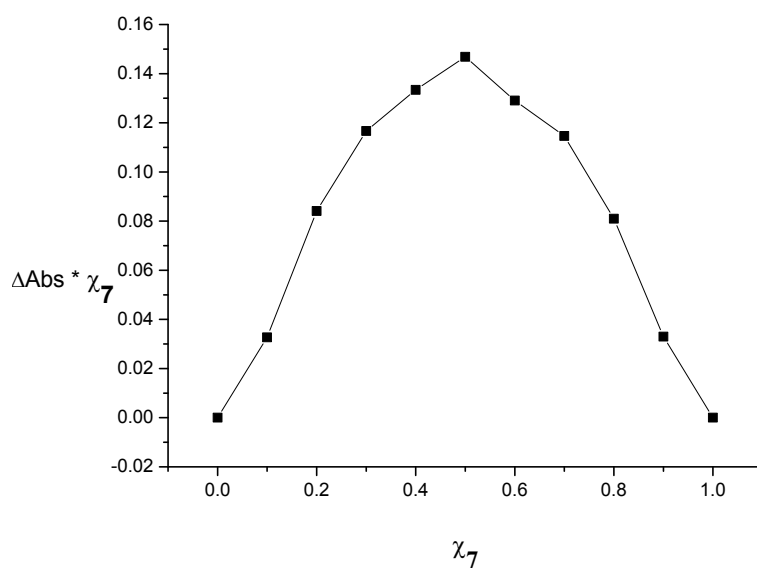


Fig. S21. Job-plot for the complex between host **7** and guest $\text{Bu}_4\text{N}^+\text{I}^-$ in CHCl_3 using UV-vis absorption value at $\lambda = 290 \text{ nm}$, showing a 1:1 stoichiometry.

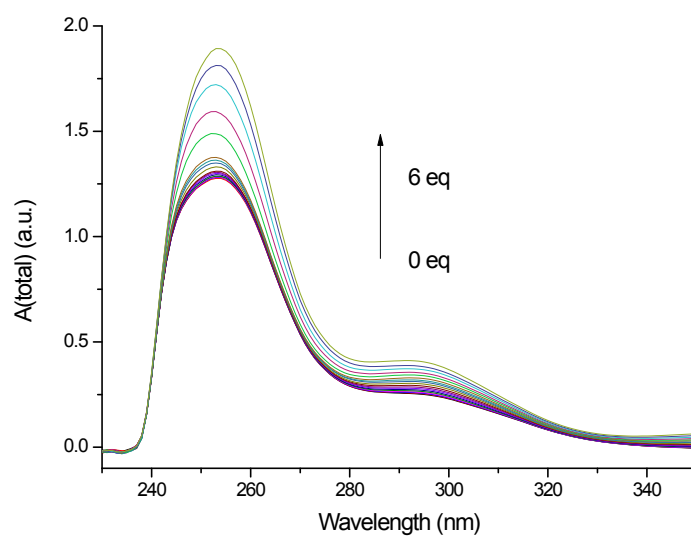


Fig. S22. Titration curves of host **7** (fixed at $2 \times 10^{-5} \text{ M}$ in CHCl_3) with 0-6 equivalents of guest $\text{Bu}_4\text{N}^+\text{I}^-$, 298 K.

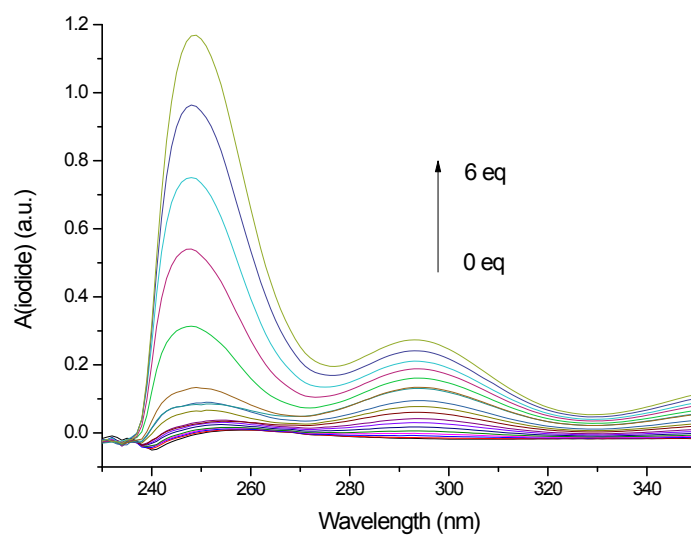


Fig. S23. UV-vis spectra of guest $\text{Bu}_4\text{N}^+\text{I}^-$ with the same concentrations in the above titration measurements.

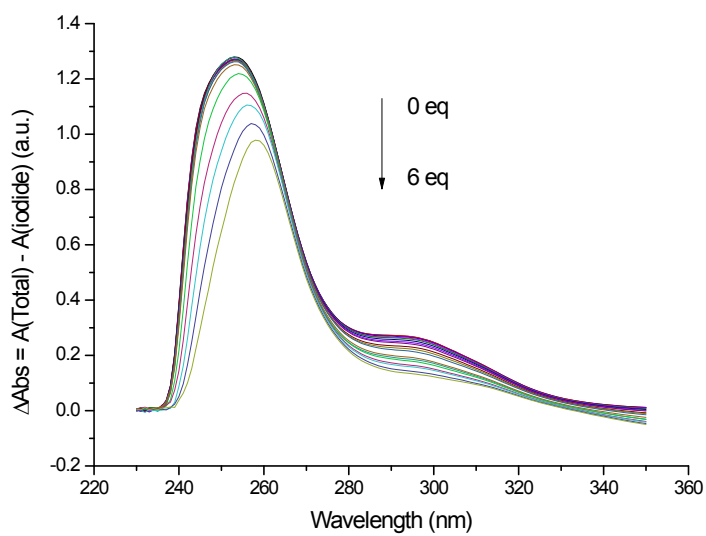


Fig. S24. UV-vis titration curves, after deduction of I^- absorbance.

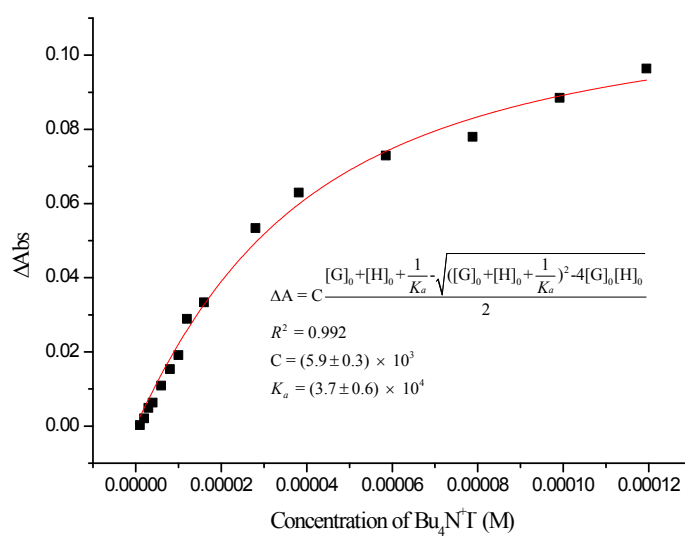


Fig. S25. Plot of the absorption intensity changes at $\lambda = 282$ nm vs the guest concentration. The red line was obtained from non-linear curve-fitting using Eq. S1, yielding an association constant $K_a = (3.7 \pm 0.6) \times 10^4 \text{ M}^{-1}$.

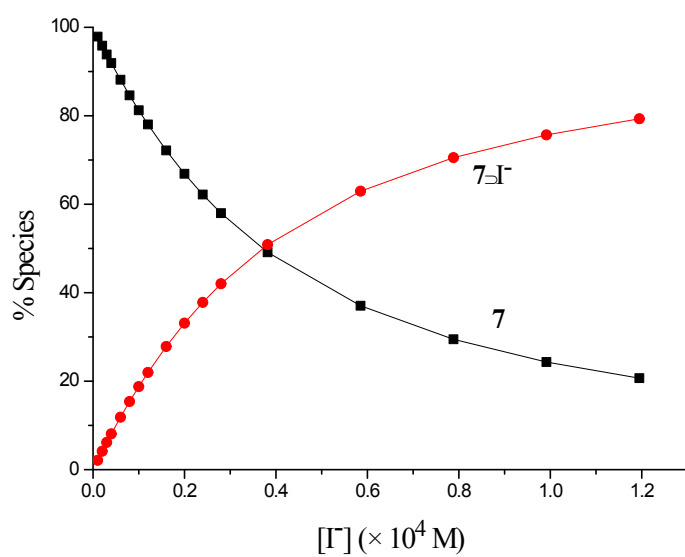


Fig. S26. Distribution diagram between **7** and **7⇌I⁻** during the spectrophotometric titration, calculated using UV-vis titration absorption data at $\lambda = 282$ nm.

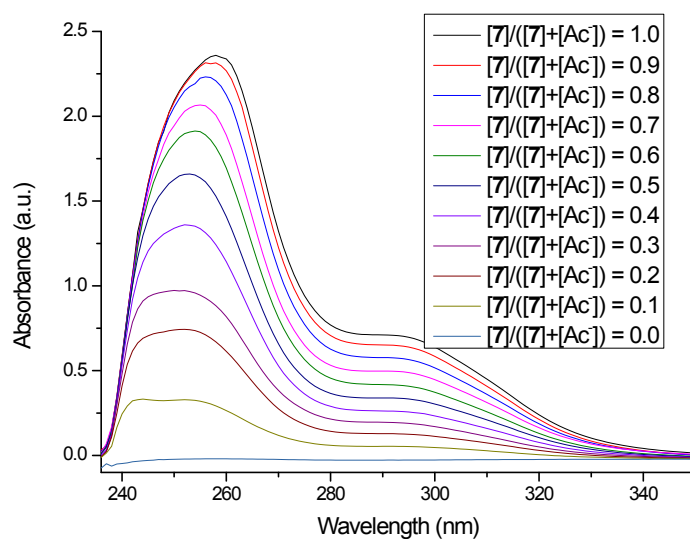


Fig. S27. UV-vis spectra of mixtures of host **7** and guest $\text{Bu}_4\text{N}^+\text{Ac}^-$ with different ratios in CHCl_3 , with the total concentration fixed at 5×10^{-5} M.

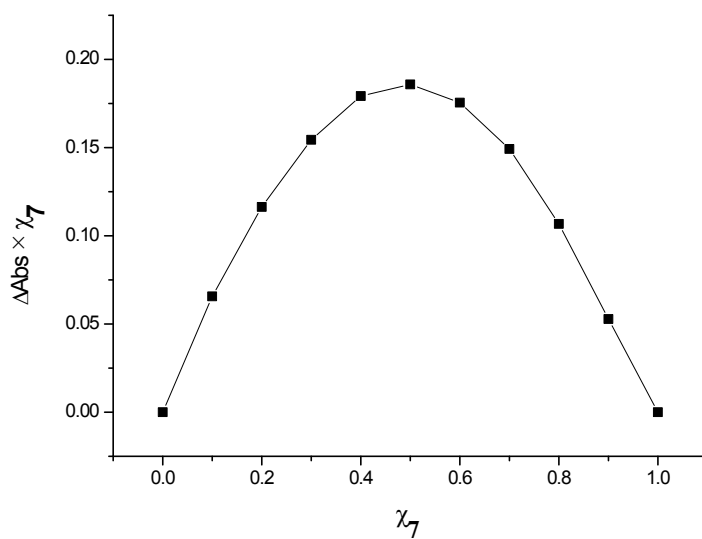


Fig. S28. Job-plot for the complex between host **7** and guest $\text{Bu}_4\text{N}^+\text{Ac}^-$ in CHCl_3 using UV-vis absorption value at $\lambda = 290$ nm, showing a 1:1 stoichiometry.

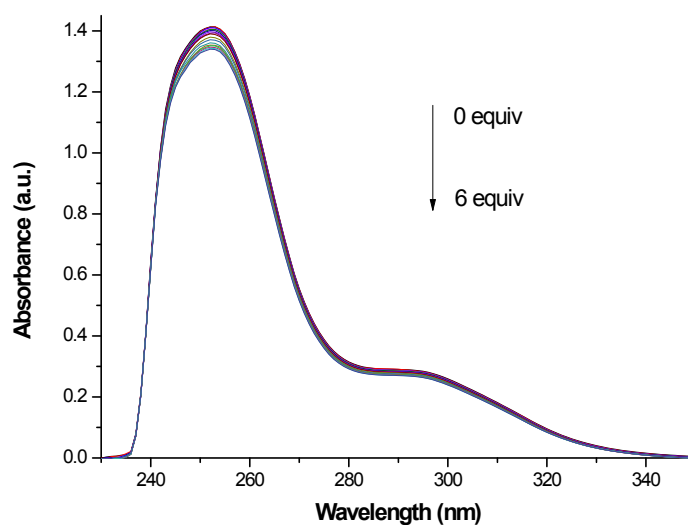


Fig. S29. Titration curves of host **7** (fixed at 2×10^{-5} M in CHCl_3) with 0-6 equivalents of guest $\text{Bu}_4\text{N}^+\text{Ac}^-$, 298 K.

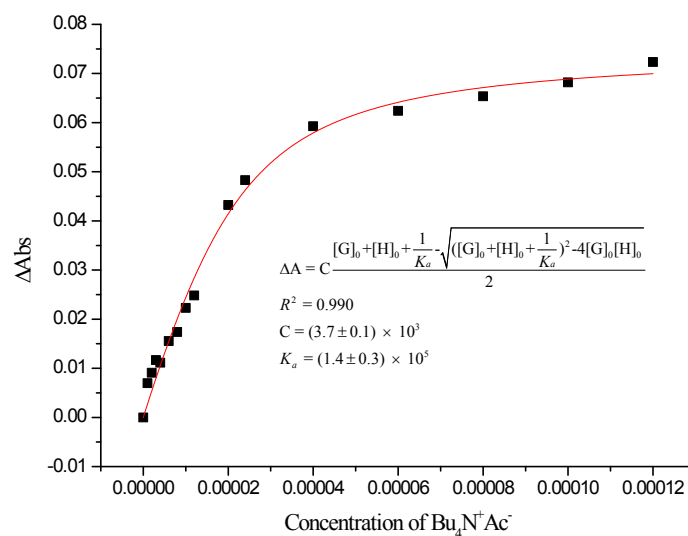


Fig. S30. Plot of the absorption intensity changes at $\lambda = 255$ nm vs the guest concentration. The red line was obtained from non-linear curve-fitting using Eq. S1, yielding an association constant $K_a = (1.4 \pm 0.3) \times 10^5 \text{ M}^{-1}$.

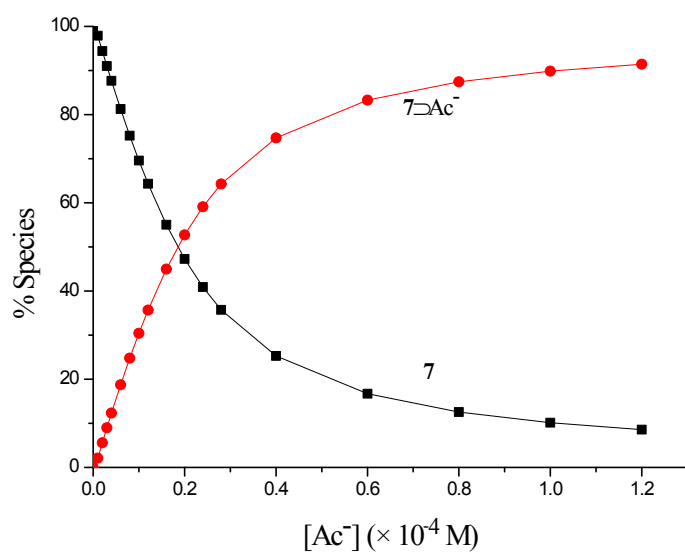


Fig. S31. Distribution diagram between **7** and **7⊃Ac⁻** during the spectrophotometric titration, calculated using UV-vis titration absorption data at $\lambda = 255$ nm.

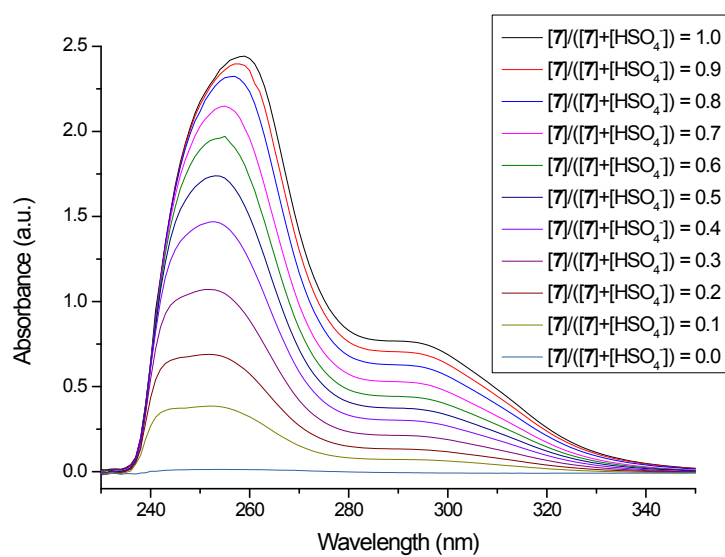


Fig. S32. UV-vis spectra of mixtures of host **7** and guest $\text{Bu}_4\text{N}^+\text{HSO}_4^-$ with different ratios in CHCl_3 , with the total concentration fixed at 5×10^{-5} M.

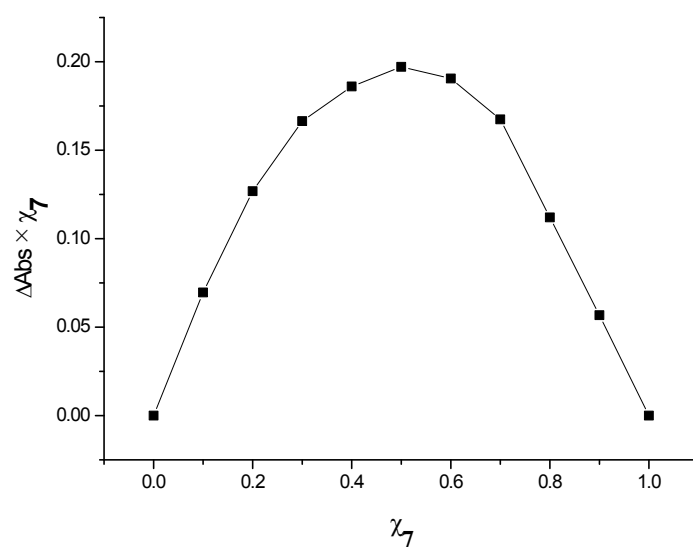


Fig. S33. Job-plot for the complex between host **7** and guest $\text{Bu}_4\text{N}^+\text{HSO}_4^-$ in CHCl_3 using UV-vis absorption value at $\lambda = 290 \text{ nm}$, showing a 1:1 stoichiometry.

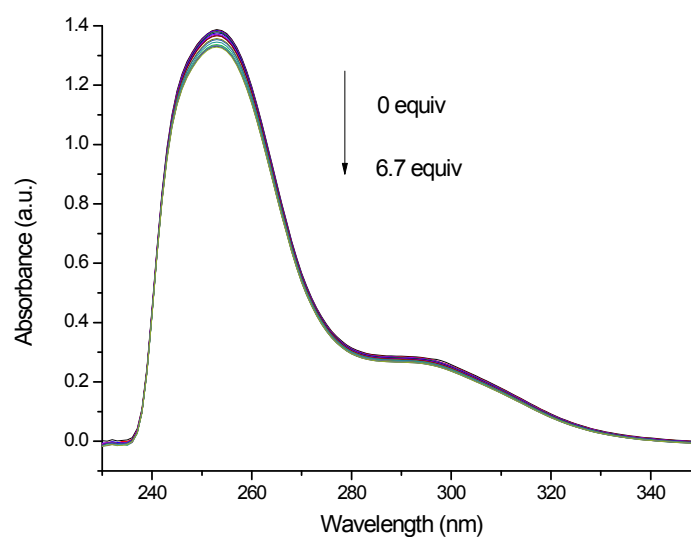


Fig. S34. Titration curves of host **7** (fixed at $2 \times 10^{-5} \text{ M}$ in CHCl_3) with 0-6.7 equivalents of guest $\text{Bu}_4\text{N}^+\text{HSO}_4^-$, 298 K.

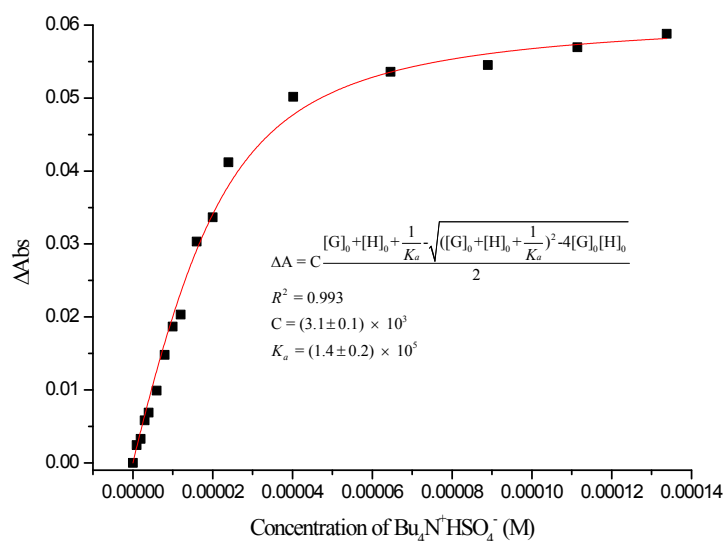


Fig. S35. Plot of the absorption intensity changes at $\lambda = 254$ nm vs the guest concentration. The red line was obtained from non-linear curve-fitting using Eq. S1, yielding an association constant $K_a = (1.4 \pm 0.2) \times 10^5 \text{ M}^{-1}$.

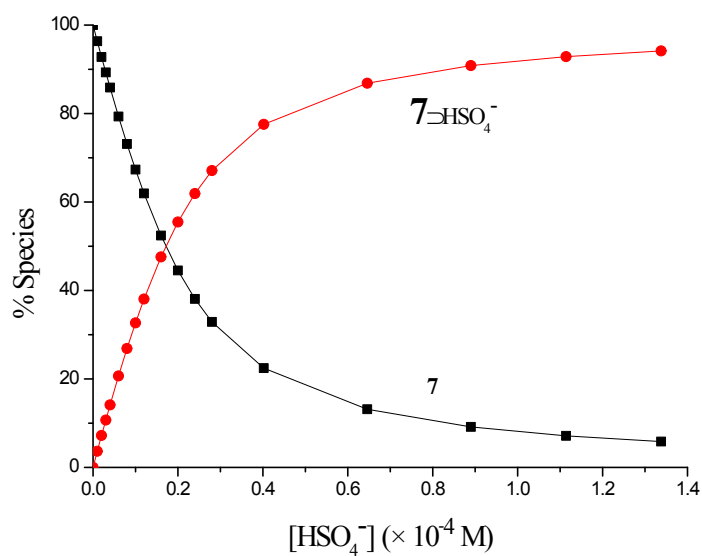


Fig. S36. Distribution diagram between **7** and **7-HSO₄⁻** during the spectrophotometric titration, calculated using UV-vis titration absorption data at $\lambda = 254$ nm.

Reference

- S1. K. A. Connors, *Binding Constants: The Measurement of Molecular Complex Stability*, Wiley, 1987
- S2. K. Hirose, in *Analytical Methods in Supramolecular Chemistry*, ed. C. Schalley, Wiley-VCH, 2012, vol. 1, pp. 27-66.